Chemistry A European Journal

Chemistry Europe
European Chemical Societies Publishing

Cover Feature:
M. O. Senge, A. Wiehe et al.
Dipyrrinato-Iridium(III) Complexes for Application in Photodynamic Therapy and Antimicrobial Photodynamic Inactivation

21/2021

WILEY-VCH

Chemistry–A European Journal
Full Paper
doi.org/10.1002/chem.202004776

Chemistry Europe
European Chemical Societies Publishing

Iridium(III) Complexes | *Hot Paper*

Dipyrrinato-Iridium(III) Complexes for Application in Photodynamic Therapy and Antimicrobial Photodynamic Inactivation

Benjamin F. Hohlfeld,[a, b] Burkhard Gitter,[b] Christopher J. Kingsbury,[c] Keith J. Flanagan,[c] Dorika Steen,[b] Gerhard D. Wieland,[b] Nora Kulak,[a, d] Mathias O. Senge,*[c, e] and Arno Wiehe*[a, b]

Dedicated to Professor Peter J. Sadler

Abstract: The generation of bio-targetable photosensitizers is of utmost importance to the emerging field of photodynamic therapy and antimicrobial (photo-)therapy. A synthetic strategy is presented in which chelating dipyrrin moieties are used to enhance the known photoactivity of iridium(III) metal complexes. Formed complexes can thus be functionalized in a facile manner with a range of targeting groups at their chemically active reaction sites. Dipyrrins with N- and O-substituents afforded (dipy)iridium(III) complexes via complexation with the respective Cp*-iridium(III) and ppy-iridium(III) precursors (dipy = dipyrrinato, Cp* = pentamethyl-η^5-cyclopentadienyl, ppy = 2-phenylpyridyl). Similarly, electron-deficient [Ir^{III}(dipy)$(ppy)_2$] complexes could be used for post-functionalization, forming alkenyl, alkynyl and glyco-appended iridium(III) complexes. The phototoxic activity of these complexes has been assessed in cellular and bacterial assays with and without light; the [Ir^{III}(Cl)(Cp*)(dipy)] complexes and the glyco-substituted iridium(III) complexes showing particular promise as photomedicine candidates. Representative crystal structures of the complexes are also presented.

Introduction

Metal complexes are widely used as catalysts in diverse chemical reactions, e.g., cross-coupling reactions,[1] oxidation reactions,[2] alkylation,[3] olefination or in olefin metathesis.[4] Beside the catalytic application, metal complexes are currently intensively investigated as therapeutically active compounds. Specifically, metal complexes are well established for chemotherapeutic treatments,[5] as contrast agents in medical imaging,[6] or as antibacterial agents.[7] In this context, iridium(III) complexes have also found interest as chemotherapeutic agents.[8] It has been shown that iridium(III) complexes can interact with specific cellular targets, for example, mitochondria, DNA, proteins, and lysosome structures.[9] Currently, metal complexes are also showing increasing promise for an application as photosensitizers in photodynamic therapy (PDT).[10] PDT is a medical treatment of cancer and other, non-malignant diseases and can serve as an alternative to classical treatments, such as surgery, chemotherapy or radiotherapy.[11] PDT uses light sensitive dyes (photosensitizers) for the destruction of cancer cells. The photosensitizer is activated by light of an appropriate wavelength in the presence of oxygen, and cytotoxic reactive oxygen species (ROS) are generated, which results in oxidative cellular damage and destruction.[11a–c, 12] In comparison to traditional chemotherapy or surgery, PDT has a number of advantages, chiefly that the specific irradiation limits the effect to the target tissue and side-effects are lessened due to weak dark toxicity of the photosensitizers and short half-life time of ROS.

[a] *B. F. Hohlfeld, Prof. Dr. N. Kulak, Dr. A. Wiehe*
Institut für Chemie u. Biochemie
Freie Universität Berlin
Takustr. 3, 14195 Berlin (Germany)

[b] *B. F. Hohlfeld, Dr. B. Gitter, D. Steen, Dr. G. D. Wieland, Dr. A. Wiehe*
biolitec research GmbH
Otto-Schott-Str. 15, 07745 Jena (Germany)
E-mail: arno.wiehe@biolitec.com
Homepage: https://www.biolitec.de/

[c] *Dr. C. J. Kingsbury, Dr. K. J. Flanagan, Prof. Dr. M. O. Senge*
Medicinal Chemistry, Trinity Translational Medicine Institute
Trinity Centre for Health Sciences
Trinity College Dublin, The University of Dublin
St James's Hospital, Dublin 8 (Ireland)
E-mail: sengem@tcd.ie

[d] *Prof. Dr. N. Kulak*
Institut für Chemie
Otto-von-Guericke-Universität Magdeburg
Universitätsplatz 2, 39106 Magdeburg (Germany)

[e] *Prof. Dr. M. O. Senge*
Institute for Advanced Study (TUM-IAS)
Technical University of Munich
Lichtenbergstrasse 2a, 85748 Garching (Germany)
E-mail: sengem@tcd.ie
Homepage: https://chemistry.tcd.ie/staff/people/mos/Home.html

Supporting information and the ORCID identification numbers for the authors of this article can be found under: https://doi.org/10.1002/chem.202004776.

Moreover, this modality can be used when other therapeutic options are exhausted or in case of specific contraindications to chemotherapy or surgery in vulnerable patient groups.[11b,c,13] In addition, *antimicrobial* photodynamic inactivation (aPDI) has significant potential for an effective inactivation of bacteria,[14] as well as viruses[15] and fungi[16] and other microbiota in vitro and in vivo.[17] In this context, iridium complexes have also been evaluated as photosensitizers for aPDI against Gram-positive and Gram-negative bacteria,[18,19] and have been found to effectively generate ROS.[18] Specifically for metal complexes, however, other phototoxic mechanisms, for example, photoinduced ligand exchange, may play an additional role.[20]

As well, in recent years, dipyrrins (dipyrromethenes) have caught attention as organic ligands for metal complexes. Dipyrrins are known to coordinate various metals, e.g., zinc, copper, gallium, platinum, palladium, iridium, and ruthenium.[21] Such complexes can exclusively consist of dipyrrins (homoleptic complexes);[22] as well, metal complexes are reported, containing a combination of dipyrrins and other organic ligands (heteroleptic complexes). Typically, *p*-cymene, η^5-cyclopentadienyl, 2-phenylpyridyl, or 2,2-bipyridyl ligands are moieties employed as capping in heteroleptic dipyrrinato complexes (Figure 1).[21b,d,23]

Dipyrrinato ligands have found interest as components for the formation of coordination polymers and supramolecular assemblies,[24] or light harvesting structures in dye-sensitized solar cells.[25] Furthermore, dipyrrinato-iridium and -ruthenium complexes show high potential for an application as chemotherapeutic agents. Specifically, ferrocene-appended (dipyrrinato)(pentamethylcyclopentadienyl)iridium(III) and (dipyrrinato)(*p*-cymene)ruthenium(II) complexes have been reported to exhibit an increased binding affinity to DNA.[23c,26] Also, dipyrrinato complexes of zinc, ruthenium and gallium show promising potential for PDT.[27]

In this work, the stepwise synthesis of chlorido(dipyrrinato)-(pentamethyl-η^5-cyclopentadienyl)iridium(III) complexes and (dipyrrinato)bis(2-phenylpyridyl)iridium(III) complexes for use in PDT and aPDI is presented. *meso*-Substituted dipyrrins, based on the pentafluorophenyl- and the 4-fluoro-3-nitrophenyl moiety, are used for the syntheses of these dipyrrinato iridium complexes. As shown previously, the pentafluorophenyl and the 4-fluoro-3-nitrophenyl moiety hold significant potential for subsequent nucleophilic substitutions on the respective *para*-fluorine position.[27a,28] Hence, the *p*-fluorine exchange with numerous nucleophiles, for example, amines and thio-carbohydrates, is applied to introduce specific functional structures. Synthesis of cyclometalated iridium complexes is performed via both the complexation of pre-functionalized dipyrrins and the post-functionalization of related pentafluorophenyl- and 4-fluoro-3-nitrophenyl-substituted dipyrrinato complexes. Crystals suitable for X-ray single-crystal structure determination were obtained for five complexes allowing for analysis of molecular structure and conformation in the solid state. To preliminarily assess the suitability of the complexes for phototherapy, the iridium complexes were evaluated for their phototoxic effect with and without light in assays against several cancer cell lines. The complexes were as well evaluated for their antibacterial effect (again with and without light) against the Gram-positive germ *S. aureus* and the Gram-negative germ *P. aeruginosa*. Moreover, instead of testing the substances in phosphate-buffered saline (PBS) only, all tests against bacteria were additionally carried out with the addition of serum, to challenge their activity under more realistic conditions. In these assays, structures with a high phototoxic potential against bacteria and cancer cells were identified, pointing at structural elements that favor an application in PDT and aPDI.

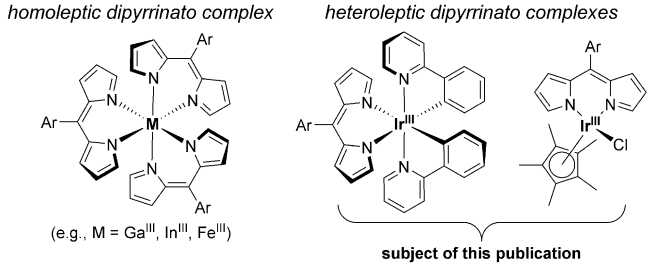

Figure 1. Examples for homo- and heteroleptic dipyrrinato complexes.

Results and Discussion

Synthesis of target compounds

Syntheses of heteroleptic metal complexes employing dipyrrinato ligands based on late transition metals, e.g., ruthenium(II), rhodium(III) and iridium(III), are known in the literature.[21a,23a,b,26a,29] The synthesis of the dipyrrinato complexes typically involves reaction of the dipyrrins under basic conditions with a commercially available (dichlorido-bridged) metal-arene precursor.[2a,b,23b,26a,27a,28d,29a,b,30]

In this work, *meso*-substituted dipyrrins based on the 5-pentafluorophenyl and the 5-(4-fluoro-3-nitrophenyl) moiety were tested for the preparation of dipyrrinato iridium(III) complexes. The pentafluorophenyl group, as well as the 4-fluoro-3-nitrophenyl group, enable subsequent nucleophilic aromatic substitution reactions (S_NAr), introducing, e.g., sugar moieties[27a,28e,31] or alkynyl groups, giving access to subsequent 1,3-dipolar cycloaddition reactions for the connection with biomolecules or polyethylene glycols ("click" chemistry).[32]

In preparation for the following experiments, the *meso*-substituted dipyrromethanes **1**–**15** were synthesized according to known procedures published by us and others.[28a,b,d,e,33] Dipyrromethanes can then be transformed into the dipyrrins via oxidation with a suitable oxidation agent.[22b,27a,28d,33,34] Here, dipyrromethanes (**1**–**15**) served as starting materials for the required dipyrrins (Scheme 1).

Previously, the oxidation of some pentafluorophenyl-substituted dipyrromethanes (namely **1**, **3**, and **5**–**7**) has been described in the literature using 2,3-dichloro-5,6-dicyano-1,4-benzoquinone (DDQ).[27a,34] Analogously, the dipyrromethanes **2** and **4** were oxidized with DDQ. Nevertheless, the observed yields were quite low (18% and 40%, respectively, for details cf. Supporting Information, S4.3.1 and S4.3.2). To achieve a

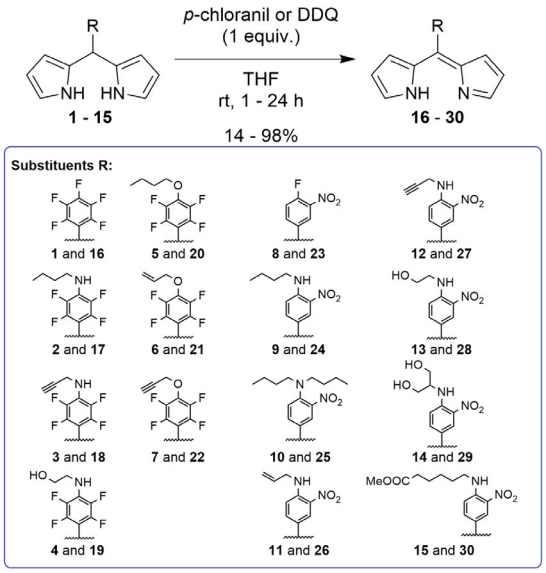

Scheme 1. Synthesis of *meso*-substituted dipyrrins via oxidation of dipyrromethanes (dipyrromethanes were synthesized according to the literature).[28a,b,d,e,33]

higher conversion into the desired dipyrrins, DDQ was replaced by *p*-chloranil which gave better yields for the oxidation of **2** and **4** (73% and 45%, respectively, for details on these reactions and the following discussion cf. Supporting Information, S4.1, S4.2, and S4.3). The dipyrromethanes **1**, **3**, **5**, and **7** were successfully oxidized with *p*-chloranil to their corresponding dipyrrins as well, again resulting in higher yields for three of the compounds compared to the literature.[27a] The exception was the pentafluorophenyl-substituted dipyrromethane **1**, here, lower yields were observed with *p*-chloranil compared to DDQ.[34]

Similarly, the *meso*-(4-amino-3-nitrophenyl)-substituted dipyrrins **24**, **25**, **27**, **29**, and **30** were prepared from the corresponding dipyrromethanes by oxidation with *p*-chloranil as already described in the literature.[28d] Based on this procedure, the dipyrrins **26** and **28** were prepared with the same oxidation reagent. Interestingly, a successful oxidation of the unsubstituted dipyrromethane **8** to dipyrrin **23** with *p*-chloranil was not possible. Here, in analogy to the conversion of **1** to **16**, DDQ was required for a successful oxidation to the desired product **23**. With DDQ as oxidizing agent, dipyrrin **23** was obtained in 81% yield. In an additional set of experiments, DDQ was tested as well for the oxidation of the other dipyrromethanes **9**–**15**. While DDQ could be used for this reaction it resulted in significantly lower yields than *p*-chloranil (see Supporting Information, S4.1, S4.2, and S4.3). Hence, we recommend the use of *p*-chloranil for this type of dipyrromethanes.

In the next step, the dipyrrins **16**–**30** were converted to the corresponding chlorido(dipyrrinato)(pentamethyl-η^5-cyclopentadienyl)iridium(III) complexes **31**–**45** (Table 1 and Table 2). The synthesis of the dipyrrinato iridium complexes required a base for the deprotonation of the dipyrrin and a suitable dichlorido-bridged iridium(III) precursor.[21a,b,26a] Hence, the pentafluorophenyl-substituted dipyrrin **16** and the pre-functionalized dipyrrins (**17**–**22**) were reacted with *N*,*N*-diisopropylethylamine (DIPEA) and the di-μ-chlorido-bis[chlorido(pentamethyl-η^5-cyclopentadienyl)iridium(III)] to obtain the desired complexes **31**–**37** (Table 1). Very high yields were observed with **16** and with the pre-functionalized dipyrrin **20** (91% and 86%, respectively); dipyrrins **17** and **19** gave the corresponding complexes in moderate yields (Table 1). The lack of formation of compounds **33**, **36**, and **37** can be explained in part by the reactivity of the respective dipyrrins **18**, **21**, and **22**, that is, those carrying an allyl or a propargyl moiety. We found hints for a cleavage of the propargyl group, e.g., in the case of dipyrrins **18** and **22**, in NMR and mass spectra, and evidence for the formation of the corresponding 4-amino-2,3,5,6-tetrafluorophenyl- and the 4-hydroxy-2,3,5,6-tetrafluorophenyl moieties (see Supporting Information, S5.4 and S5.8).

Table 1. Synthesis of chlorido(dipyrrinato)(pentamethyl-η^5-cyclopentadienyl)iridium(III) complexes with dipyrrins **16**–**22**.

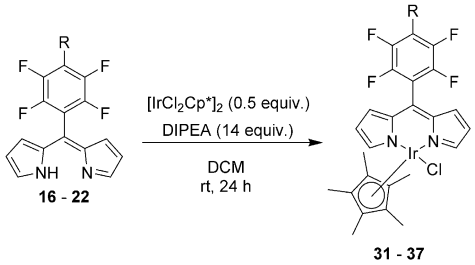

Entry	Starting material	Substituent (R)	Product	Yield [%]
1	**16**		**31**	91
2	**17**	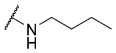	**32**	36
3[a,b]	**18**	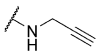	**33**	
4	**19**	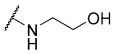	**34**	36
5	**20**	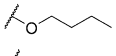	**35**	86
6[a]	**21**	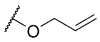	**36**	
7[a,b]	**22**	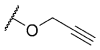	**37**	

[a] No product was observed. [b] Evidence for a dealkylation of the propargyl group was found (see Supporting Information, sections S5.4 and S5.8).

Using the same method, the synthesis of chlorido(dipyrrinato)(pentamethyl-η^5-cyclopentadienyl)iridium(III) complexes, based on the related 3-nitrophenyl-substituted dipyrrins **23**–**30**, was performed. Again, the dipyrrins were reacted with DIPEA and the di-μ-chlorido-bis[chlorido(pentamethyl-η^5-cyclopentadienyl)iridium(III)] to obtain the corresponding complexes **38**–**45**. (Table 2). For the dipyrrins **23**, **24**, and **27**–**30**, the reactions led to the desired complexes (**38**, **39**, and **42**–**45**) in moderate to good yields (Table 2). With the dipyrrins **40** and **41**—functionalized with an allyl group or a propargyl group—formation of the corresponding metal complexes was not observed; instead inseparable mixtures of multiple products were

Table 2. Synthesis of chlorido(dipyrrinato)(pentamethyl-η^5-cyclopentadienyl)iridium(III) complexes with dipyrrins **23**–**30**.

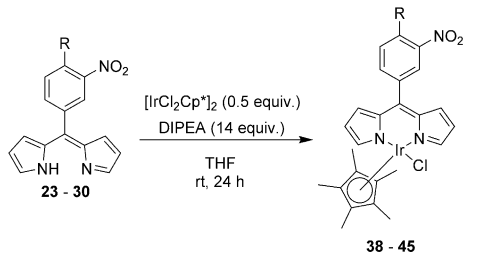

Entry	Starting material	Substituent (R)	Product	Yield [%]
1	**23**		**38**	43
2	**24**	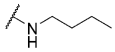	**39**	46
3[a]	**25**	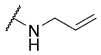	**40**	
4[a]	**26**	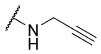	**41**	
5	**27**	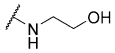	**42**	46
6	**28**	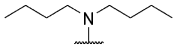	**43**	29
7	**29**	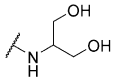	**44**	29
8	**30**	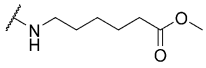	**45**	52

[a] No product was observed.

obtained. Here, no evidence for a dealkylation of the allyl or the propargyl group could be found. In order to generate the allyl or propargyl functionalized complexes (namely **33**, **36**, **37**, **40**, and **41**) the synthetic procedure was modified. The unfunctionalized complexes **31** and **38** were tested for possible subsequent nucleophilic substitutions; complex **31** was reacted with amines and alcohols, e.g., propargylamine, propargyl alcohol, or allyl alcohol (for details on these reactions and the following discussion cf. the Supporting Information, S6). Similar reactions were performed with complex **38** except for the reaction with alcohols, infeasible due to known side reactions of the alkoxide with the nitro group.[28d] Absorption spectra of selected chlorido(dipyrrinato)(pentamethyl-η^5-cyclopentadienyl)iridium(III) complexes are presented in the Supporting Information, section S13.

A post-functionalization of tris(pentafluorophenyl)dipyrrinato complexes with amines and alcohols has been described in the literature.[27a] However, the trial reactions with **31** and **38** were unsuccessful (see Supporting Information, S6), probably due to ligand exchange reactions. An exception was the substitution of **38** with *n*-butylamine, where the desired complex **39** was isolated with 71% yield. In the case of the post-functionalization of **31** with allyl alcohol, the NMR spectrum again provided evidence for the formation of the corresponding 4-hydroxy-2,3,5,6-tetrafluorophenyl moiety.

The complications in the syntheses described above occurred mainly with complexes carrying double and triple bonds. The observed cleavage of the allyl and propargyl group might be caused by interactions of the iridium with these multiple bonds. Such interaction of multiple bonds and metal complexes typically occurs in metathesis reactions or alkene and alkyne rearrangements, both reactions where iridium-based catalysts have been employed.[35,36]

The introduction of additional functional groups to the pyrrole units of the dipyrrin chelate is a further means to modulate the (photo)chemical characteristics of the resulting metal complex.[27b,37] Hence, we investigated the synthesis of chlorido(dipyrrinato)(pentamethylcyclopentadienyl)iridium(III) complexes with dipyrrins carrying additional methyl groups at the 1-,3-,7-, and 9-position. For this, the 5-pentafluorophenyl-1,3,7,9-tetramethyldipyrrin **48** and the 5-(4-fluoro-3-nitrophenyl)-1,3,7,9-tetramethyldipyrrin **49** were tested in the synthesis of cyclometalated iridium complexes. The synthesis of dipyrrin **48** has previously been described in the literature.[38] However, **48** was originally prepared in a one-pot multi-step synthesis from 2,4-dimethylpyrrole and pentafluorobenzaldehyde. In this work, we opted for a stepwise synthesis of the corresponding 1,3,7,9-tetramethyl dipyrrins **48** and **49**. This would also enable future nucleophilic substitutions already at the dipyrromethane stage following on from the previous experiments (see above) which have shown that the use of pre-substituted dipyrrins is more effective in the synthesis of chlorido(dipyrrinato)(pentamethylcyclopentadienyl) complexes.

The 1,3,7,9-tetramethyl substituted dipyrromethanes **46** and **47** were prepared via trifluoroacetic acid-catalyzed condensation of 2,4-dimethylpyrrole and the corresponding benzaldehyde (pentafluorobenzaldehyde or 4-fluoro-3-nitrobenzaldehyde). The respective dipyrromethanes were obtained in almost quantitative yields (Scheme 2). In the next step, the corresponding dipyrrins **48** and **49** were formed via oxidation with DDQ and isolated in 63% and 90% yield, respectively (Scheme 2). Compared to the literature,[38] the stepwise synthesis of dipyrrin **48** provided no significant difference in the overall yield.

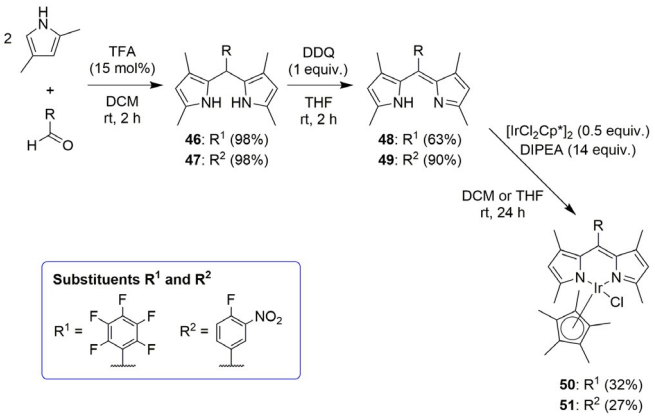

Scheme 2. Synthesis of chlorido(pentamethylcyclopendadienyl)(1,3,7,9-tetramethyldipyrrinato)iridium(III) complexes.

Finally, the target dipyrrinato iridium complexes **50** and **51** were synthesized, employing the method described for the preparation of the previous chlorido(dipyrrinato)(pentamethylcyclopentadienyl)iridium(III) complexes that is, deprotonation with DIPEA, followed by complexation with the corresponding metal precursor. Complexes **50** and **51** could be obtained in 32% and 27% yield, respectively (Scheme 2). The low yields may be the result of partial decomposition of the starting material, as evidenced by the formation of a large amount of a black precipitate during the reactions.

Another type of heteroleptic dipyrrinato iridium(III) complexes is represented by (dipyrrinato)bis(2-phenylpyridyl)iridium(III) systems.[23a,29b,30] Related bis(2,2′-bipyridyl)(dipyrrinato)ruthenium(II) complexes have been synthesized previously via the ligand exchange of corresponding chlorido(*p*-cymene)(dipyrrinato)ruthenium(II) complexes with 2,2′-bipyridine.[27a,28d] Analogously, complexes **31** and **43** were tested in ligand exchange reactions with 2-phenylpyridine. Complex **31** was dissolved together with 2-phenylpyridine in ethanol and was reacted under reflux. Alternatively, the ligand exchange of **43** was performed in a 1-methoxyethanol/water mixture, to increase the reaction temperature. However, in both cases the desired products (**52** and **53**) could not be obtained and the starting materials were recovered (see Supporting Information, S7.1 and S7.2).

Thus, to obtain the desired (dipyrrinato)bis(2-phenylpyridyl)iridium(III) complexes the synthetic procedure had to be modified. The synthesis of the target systems was performed via the complexation of dipyrrins with bis(μ-chlorido)tetrakis(2-phenylpyridyl)diiridium(III).[23a,29b,c,30] For this, the dipyrrins (**16**–**22**) were reacted with DIPEA and bis(μ-chlorido)tetrakis(2-phenylpyridyl)diiridium(III) in THF to obtain the corresponding complexes (**52**, **54**–**59**, Table 3). The highest yield, 65%, was achieved with dipyrrin **16**. The reactions with pre-functionalized dipyrrins (**17**, **19**–**21**) also gave the desired complexes (**52**, **54**, **56**, and **57**) in good yields (Table 3). Again, for dipyrrins with the propargyl moieties (**18** and **22**) no product was obtained. Also, the allyl-substituted complex **58** could only be isolated in 8% yield (Table 3) via the complexation with dipyrrin **21**. In the case of complex **55**, the NMR spectrum provided evidence for a dealkylation of the propargylamino group (see Supporting Information, S8.4).

In the next step, the 3-nitrophenyl-substituted dipyrrins **23**–**30** were tested in the synthesis of the cyclometalated iridium complexes (**53**, **60**–**66**, Table 4). Reactions with the dipyrrins **23**, **24** and **27**–**30** led to the desired complexes (**53**, **60**, **61**, and **64**–**66**) in moderate to good yields (Table 4). Using **25**—the dipyrrin carrying the allyl group—the desired complex **62** was obtained only in low yields (Table 4). In the case of complex **63**, formation of the corresponding metal complexes was not observed instead inseparable mixtures of compounds were obtained again.

In order to finally generate (dipyrrinato)bis(2-phenylpyridyl)iridium(III) complexes functionalized with an allyl group or a propargyl group, a post-functionalization approach was investigated (Schemes 3 and 4). Amines and alcohols were tested for the nucleophilic substitution of **52**, e.g., allylamine, propargyla-

Table 3. Synthesis of (dipyrrinato)bis(2-phenylpyridyl)iridium(III) complexes with dipyrrins **16**–**22**.

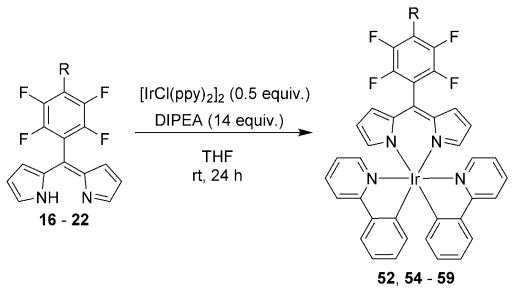

Entry	Starting material	Substituent (R)	Product	Yield [%]
1	**16**		**52**	65
2	**17**	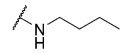	**54**	33
3[a,b]	**18**	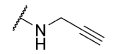	**55**	
4	**19**	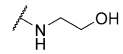	**56**	35
5	**20**	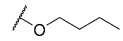	**57**	48
6	**21**	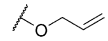	**58**	8
7[a]	**22**	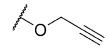	**59**	

[a] No product was observed. [b] Evidence for a dealkylation of the propargyl group was found (see Supporting Information, section S8.4).

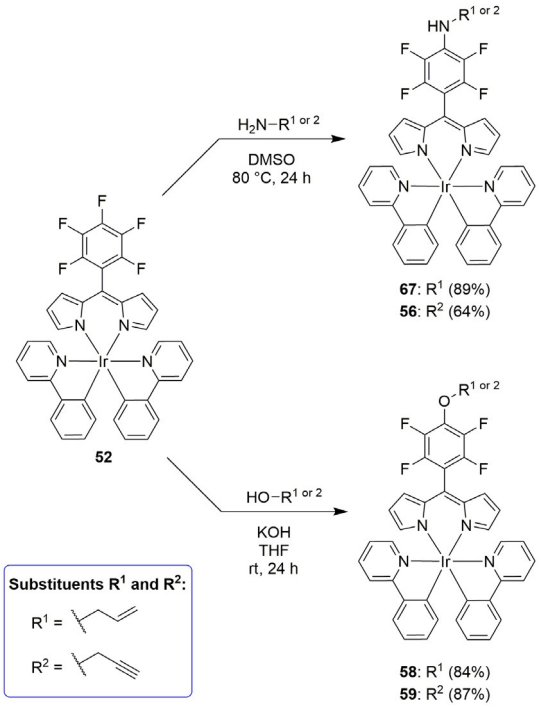

Scheme 3. Nucleophilic substitutions of complex **52** with amines und alcohols.

Table 4. Synthesis of (dipyrrinato)bis(2-phenylpyridyl)iridium(III) complexes with dipyrrins **23**–**30**.

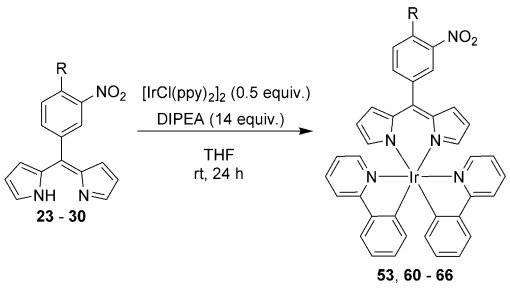

Entry	Starting material	Substituent (R)	Product	Yield [%]
1	**23**		**60**	29
2	**24**	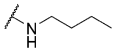	**61**	36
3	**25**		**62**	11
4[a]	**26**		**63**	
5	**27**		**64**	44
6	**28**	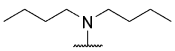	**53**	49
7	**29**	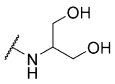	**65**	26
8	**30**	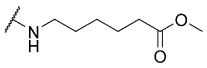	**66**	43

[a] No product could be observed.

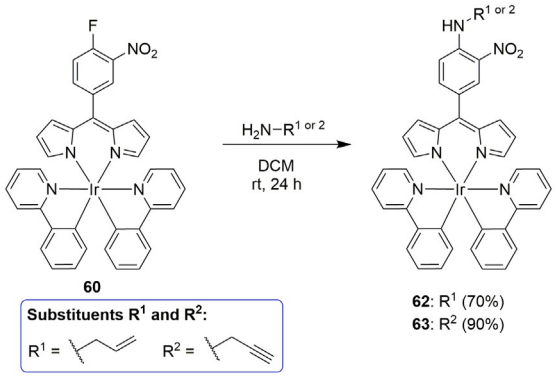

Scheme 4. Nucleophilic substitution of complex **60** with amines.

mine, allyl alcohol, and propargyl alcohol. First, complex **52** was dissolved with the corresponding amine in DMSO and stirred for 24 h at 80 °C. The desired complexes **56** and **67** could be obtained in 89% and 64% yield, respectively (Scheme 3). Substitution of **52** with allyl alcohol and propargyl alcohol was possible as well: Compound **52** was reacted with the corresponding alcohols and potassium hydroxide for the deprotonation of the alcohol to give the target systems **58** and **59** in high yields (84% and 87%, respectively, Scheme 3).

Next, complex **60** was functionalized with allylamine and propargylamine. This entailed dissolving complex **60** with the corresponding amine in DCM and gave **62** and **63** in high yields (Scheme 4). The results clearly show that the synthesis of the complexes carrying propargyl groups and allyl groups which was not possible using pre-functionalized ligands or complexes is easily viable via a post-functionalization of the unsubstituted complexes **62** and **63**. In this case, the metal center is shielded by the ligand and possible interactions with the propargyl group and allyl group are suppressed. This post-functionalization of the metal complex is thus an effective strategy circumventing the reactivity associated with ligand exchange. Absorption spectra of selected (dipyrrinato)bis(2-phenylpyridyl)iridium(III) complexes are presented in the Supporting Information, section S13.

Finally, the unsubstituted iridium complexes **52** and **60** were tested for the glycosylation with thio-carbohydrates. Glycosylation is a straightforward method to improve solubility, biological activity and bioavailability of therapeutically interesting molecules.[39] Also for iridium(III) complexes certain glycosylated derivates have been reported.[40] Different concepts for the introduction of carbohydrates have been described in the literature. On the one hand, linker groups are often used for coupling carbohydrates with therapeutically interesting molecules, e.g., BODIPY-carbohydrate conjugates, glycopeptides, or multivalent glycoconjugates.[41] Alternatively, a fast and effective method for direct glycosylation of porphyrins, corroles, and metal complexes employs an S_NAr strategy.[31,42] Notably, this type of glycosylation is feasible with unprotected thio-carbohydrates, as shown for porphyrinoids, metal complexes, and BODIPYs.[27a,28e,42a,43]

In analogy to earlier studies,[14a,28e,42a,43] the glycosylation was tested directly with unprotected thio-carbohydrates and the complexes **52** and **60**. The respective complex was dissolved in DMF together with the corresponding sodium 1′-thio-β-D-carbohydrate (glucose or galactose). Starting with **52**, within a short reaction time the corresponding glycosylated complexes (**68** and **69**) were formed (Scheme 5). The glucosyl conjugate **68** was obtained in almost quantitative and the galactosyl conjugate **69** in 92% yield. Analogous reactions of complex **60** gave the corresponding glycosylated conjugates **70** and **71** in very high yields of 92% and 90%, respectively (Scheme 5).

Conjugates of iridium(III) complexes and BODIPYs with promising photochemical properties have already been described in the literature; in this context, iridium(III)-BODIPY conjugates exhibited potential for an application as photosensitizers.[44] However, thus far, (dipyrrinato)iridium(III)-BODIPY conjugates are unknown. Here, a coupling of a BODIPY with a (dipyrrinato)iridium(III) complex was performed via the copper-catalyzed 1,3-dipolar cycloaddition. Alkynyl-substituted compounds are suitable building blocks in this reaction, e.g., for coupling porphyrins or BODIPYs to other compounds or surfaces.[28a,32c,45] Therefore, after finally having alkynyl-substituted iridium(III) complexes at hand, the 4-propargyloxy-substituted complex **59** was tested in the copper-catalyzed cycloaddition. The 4-azido substituted BODIPY **72** and the complex **59** were

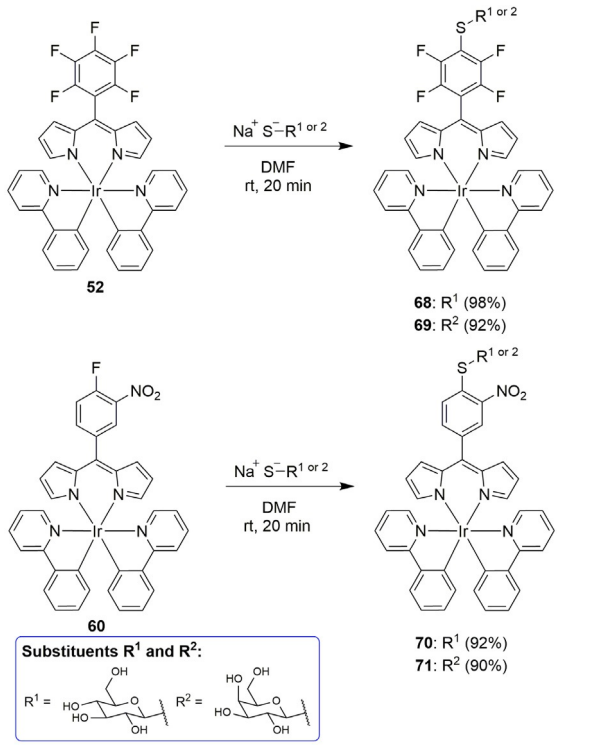

Scheme 5. Glycosylation of **52** and **60**.

dissolved in DMF and reacted with $CuSO_4$ and sodium ascorbate and gave the desired (dipyrrinato)iridium(III)-BODIPY conjugate **73** in 21% yield (Scheme 6).

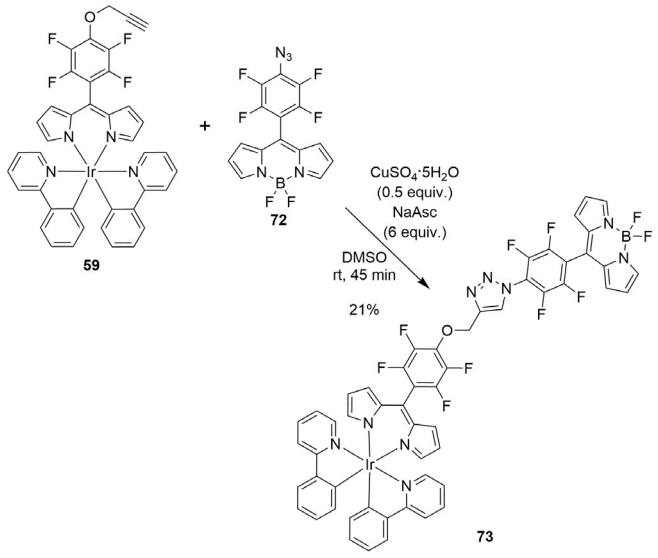

Scheme 6. Synthesis of the (dipyrrinato)iridium(III)-BODIPY conjugate **73**.

Crystal/molecular structures of dipyrrinato iridium complexes

Diffraction data for the crystal structure determinations of representative compounds of each of the classes of iridium(III) complexes were collected and refined. Two examples of the Cp* complexes are demonstrated, compounds **31** and **51**, as well as three examples of the bis(2-phenylpyridinyl) complexes **54**, **60** and **66**.

Compound **31** crystallized in a triclinic cell setting, and the solution to the diffraction pattern in P-1 is shown in Figure 2 and S1.2.1. In this complex, a lone iridium(III) metal center is coordinated by a 5-pentafluorophenyl-2,2′-dipyrrinato (N,N)-chelate, by the Cp* ligand and a single chloride. The coordination environment is the expected piano-stool geometry,[46] and approximates the Cl and N,N occupying three adjacent corners of an octahedron with interior angles of 87.14(8)°, 87.96(8)° and 85.35(12)°; the Cp* occupies the center of the opposing face.

The measured Ir-Cp* 5-atom centroid distance, at 1.7942(15) Å, is typical of iridium(III) compounds with the Cp-Cl-N^2 coordination environment (1.789(17) Å, $n = 252$).[47] The C_5 ring atoms within the Cp* ligand have a pattern of alternating longer and shorter bonds, indicating that the anionic charge is partially localized to the three carbon atoms sharing the dipyrrinato-Ir coordination plane (C17–C19).

The dipyrrin ligand is coordinated in an off-axis manner, as demonstrated in Figure 2b, such that the metal center is deviated from the mean plane of the N-C_3-N chelate by 0.600(4) Å. Discounting the 5-aryl substituent, the ligand-metal 10-atom unit has an approximate mirror plane which relates the two pyrrole subunits, with bond distances indicative of charge delocalization nearly evenly across these two pyrroles. The torsion angles around the C_α–C_{meso} bonds linking these pyrrole units (i.e. N1-C4-C5-C6 and C4-C5-C6-N2) are −0.8(6)° and 6.5(6)°, indicating a small rotational perturbation of the individ-

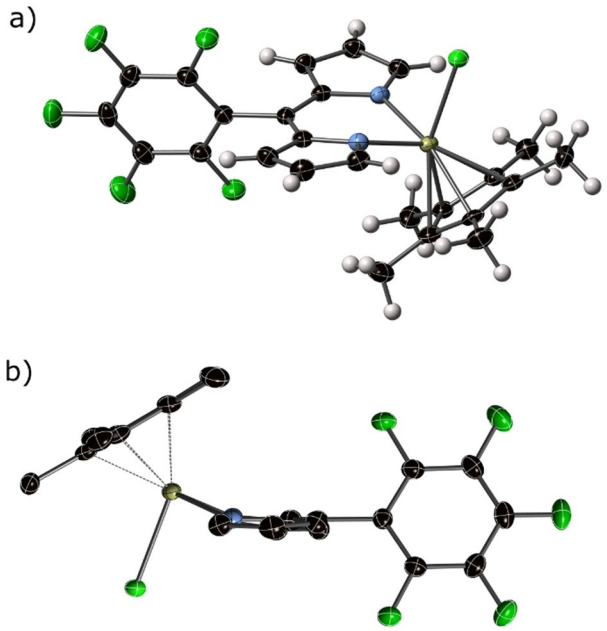

Figure 2. a) View of the structure of the asymmetric unit of compound **31** in the crystal. H atoms are represented as spheres of fixed radius, thermal ellipsoids for non-H atoms are presented at 50% probability. b) A side-on view of compound **31**, showing the off-axis coordination mode.

ual pyrrole units towards coplanarity with the Ir center. The C_6F_5 ring at the sole *meso*-position is inclined at 74.13(10)° to the mean plane of the ligand—this angle has been shown to be important in fine-tuning of the related BODIPY photochemistry.[28e,48]

The crystal structure of the related compound **51** is shown in Figure 3 and S1.2.2 and shows an iridium(III) metal center in a similar piano-stool half-sandwich coordination environment as that for **31**. Four methyl groups present on the dipyrrin moiety can be implicated in an increased distortional profile—the planar deviation (NC_3N···Ir, 0.935(5) Å), Ir···Cp* distance (1.840(2) Å) and torsion angles (C_α–C_{meso}, 2.6(5)° and 9.7(7)°) are exaggerated from the unsubstituted dipyrrin parent, with the N···N distance of the dipyrrinato chelate reduced to 2.767(5) Å, and the N–Ir distances shortened to 2.065(4) and 2.081(4) Å. The angle of the dipyrrinato mean plane to the *meso*-appended aryl unit is approximately equal to that in **31**, at 74.47(13)°. The increased steric bulk of the tetramethyl groups is sufficient to explain the distortion patterns—a pincer-like convergence of the two pyrrole units around the C_m "pivot" upon increased steric bulk has a direct effect on the coordination environment provided by the ligand. This concerted movement of the pyrrole units towards each other similarly engenders increased non-planar distortion of the dipyrrin attempting to satisfy the idealized coordination environment of the metal center.

Three previously structurally characterized examples of Ir^{III}(Cl)(Cp*) dipyrrin complexes have been reported; with a mononuclear dipyrrin,[49] a dinuclear bis-bidentate dipyrrin[50] and a macrocyclic tetrakis(perfluorophenyl)rubyrin derivative.[51] Each of these structures indicated a significant non-planarity of the iridium(III) to the dipyrrin subunit, localized piano-stool Cp* ligand atom positions and delocalization of the dipyrrin ligand electron density, in line with the two structures reported here. As has been previously reported, the coordination geometry of the iridium(III) center is particularly important for anticancer activity—presence of an exocyclic linkage of the Cp* ligand led to increased anticancer activity.[52] This 'tethering' approach inhibits hydrolysis and induces a strained coordination environment; steric conflict between α-methyl groups and the Cp* ligand strains this coordination environment in a similar manner, and is a useful tool for microstructure manipulation. We can reasonably extrapolate that each of the compounds reported herein for which a crystal structure has not been reported should adopt a similar geometry, given the limited electronic or steric influence of alteration of the terminal aryl C-F unit in each of the examples, and consistency between examples. Preliminary investigation of a crystal of compound **35** from toluene (oP, **a** 13.947(6) **b** 22.654(9) **c** 16.534(6)) has indicated a similar coordination environment is present in this example, however, data were not satisfactory for publication.

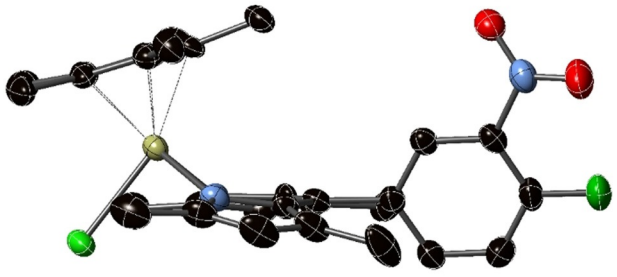

Figure 3. A view of the main molecular fragment within the crystal structure of compound **51**; thermal ellipsoids are presented at the 50% probability level. H atoms have been omitted for clarity.

Three crystal structure models, **54**, **60**·$^1/_2$**(DCM)** and **66**·$^1/_2$**(Tol)**, could be identified containing the second PDT motif, that of bis(κ^2-2-phenylpyridinyl)Ir^{III} with a substituted 5-phenyldipyrrin. Each of these structures shows the iridium(III) metal center in an octahedral C_2N_4 coordination environment, with the C atoms of the coordination environment occupying the octahedral sites *trans* to the dipyrrin. These tris-chelate compounds exhibit the expected Δ and Λ stereoisomerism, however, each was modelled as a racemate in an achiral space-group; these crystals demonstrate equal appearance of the two enantiomeric forms, in contrast to the achiral piano-stool complexes. The exclusive formation of the *trans*-pyridyl isomer is as expected for iridium compounds with the $(CN)_2(NN)$ coordination geometry, and unaltered from the presumptive geometry of the starting material;[53] the metal center geometry and bond distances are approximately equal between each of the three examples. The dipyrromethene ligand is approximately coplanar with the iridium(III) metal center in **54**, **60** and **66**, as distinct from the off-axis coordination mode observed for the piano-stool compounds **31** and **51**.

Compound **60** is shown in Figure 4b and S1.2.4; the phenylpyridine ligands and metal center exhibit the expected geometry, however, a small deviation from the idealized C_{2v} symmetry can be observed for the dipyrrin fragment indicative of contribution of partial charge localization. The aryl unit at the 5-position of the dipyrrin is inclined at 69.0°, in line with unsubstituted 5-aryl-dipyrromethene chelates (median 62.8°, IQR 55–71°, $n = 430$).

The presence of long-chain alkyl groups at the aryl 4-position in compounds **54** and **66** introduces these additional chemical motifs with retention of the metal chelate structure, as shown in Figure 4a,c, S1.2.3 and 1.2.5. The terminal alkyl chain at the aryl 4-position in **54** has higher thermal displacement as atoms process further from the aryl ring. The 4-alkylamino-substituted compound **66** exhibits an intramolecular hydrogen bond between the amine and *ortho*-nitro unit on the 5-aryl substituent, at 2.642(3) Å N···O and 129(3)° N–H···O, consistent with 2-nitroanilines generally.[54] This H-bond, expected to be present in each compound with the *o*-NH moiety is presumably responsible for the decreased thermal displacement associated with rotational averaging of the nitro unit in **60**. Previously characterized examples of $Ir(ppy)_2$(5-aryl-dipyrrin) complexes include aryl = phenyl,[30] 4-pyridyl (and derivatives thereof),[55] 4-benzoic acid (and derivatives thereof),[56] 4-(3,5-lutidinyl), 4-(*N*,*N*-diphenylamino)phenyl[30] and 4-(dimesitylborophenyl).[30,57] Each exhibited a similar coordination mode and metal-ligand distances as the structures presented above, unperturbed by peripheral modification of the aryl unit.

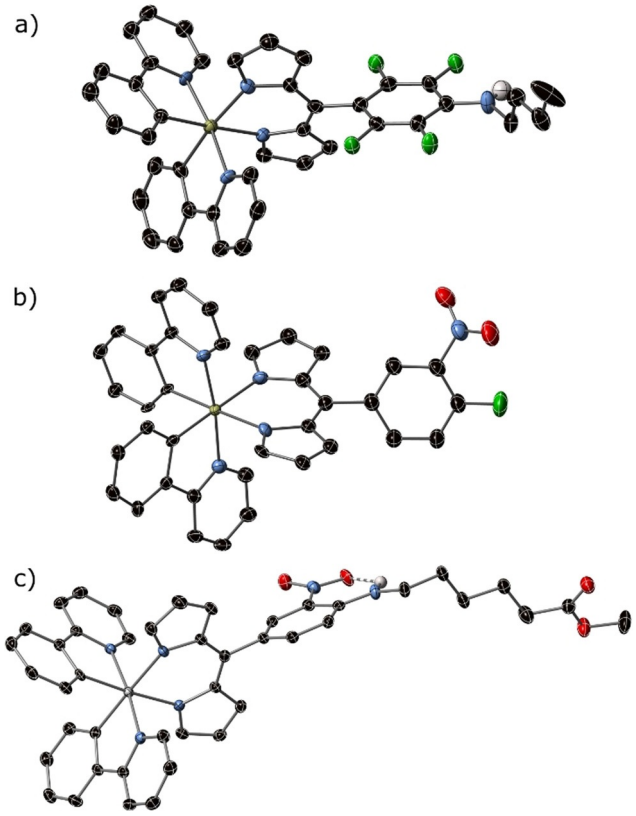

Figure 4. The main molecular units of complexes [Ir(ppy)$_2$(R-dipyrrin)] (a) **54**, R = 2,3,5,6-F$_4$-4-NHBu-Ph; (b) **60**, R = 4-F-3-NO$_2$-Ph; (c) **66**, R = 4-NHPent-CO$_2$Me-3-NO$_2$-Ph. C-bound H atoms have been omitted, and thermal ellipsoids are shown at the 50% probability level.

Evaluation in assays against bacteria and human cancer cells

The biological activity of the chlorido(dipyrrinato)(pentamethylcyclopentadienyl) iridium(III) complexes (**31**, **32**, **34**, **35**, **38**, **39**, **42**–**45**, **50**, and **51**) and the (dipyrrinato)bis(2-phenylpyridyl) iridium(III) complexes (**52**–**71**) was evaluated with and without illumination in cellular assays in four cancer cell lines. In the cellular assays the following cell lines were used: human colorectal adenocarcinoma (HT29), human epidermoid carcinoma (A431), submaxillary salivary gland epidermoid carcinoma (A253), human epithelial tongue squamous cell carcinoma (CAL27). Results for the A431 and HT29 cell lines can be seen in Figures 5–7 (for CAL27 and A253, see Supporting Information, S3.3, and S3.4). As well, the antimicrobial properties of the synthesized complexes with and without light were studied against the Gram-positive germ *S. aureus* and the Gram-negative germ *P. aeruginosa* (Figures 8–10, and Supporting Information, S3.5, S3.6).

In the cancer cell assays, cells were incubated with cell medium containig 10% fetal calf serum (FCS) and with 2 or 10 μM of the corresponding iridium complex for 24 h before irridiation. After exchange of the medium to remove any complex not taken up by the cells, a white light source at a dose rate of approximately 50 J cm^{-2} was used for irradiation. Afterwards, cells were incubated in a humidified incubator (5% CO_2 in air at 37 °C) for 24 h until cell viability assay.

As can be seen in Figure 5 (see also Supporting Information, S3.3) the chlorido(dipyrrinato)(pentamethylcyclopentadienyl)iridium(III) complexes (**31**, **32**, **34**, **35**, **38**, **39**, **42**–**45**, **50**, and **51**) in general showed no or only a low toxic effect without illumination, except for **31** and **39** in two cell lines (A431, for A253 see Supporting Information, S3.3). Under irradation with light, however, several complexes with a signifcant phototoxicity could be identified. Especially, complexes substituted with a butylamino, a butyloxy, or the dibutylamino group (**32**, **35**, **39**, and **43**) exhibited a high phototoxic effect. Also, the unfunctionalized complex **31** exhibited a high phototoxic effect on the cells, but also dark toxicity in the highest concentration. In the case of the 2,3,5,6-tetrafluorophenyl-based complexes **32** and **35**, already at a concentration of 2 μM a significant decrase of the cell viability was observed.

In comparison, the 3-nitrophenyl-substituted dipyrrinato complexes **39** and **43** showed a lower phototoxic activity. However, complex **43** still showed a phototoxic effect against all cell lines at the highest concentration; while complex **39** only exhibits phototoxicity against the cell line A253 at the highest concentration. Moreover, complex **39** showed significant dark toxicity at 10 μM against the cell line A253 (see Supporting Information, S3.3).

Interestingly, the complexes **32**, **42**, and **44**, functionalized with polar groups, generally showed only a limited phototoxic activity. Only complex **42** showed a higher phototoxic effect on specific cell lines (A431, for CAL27 see S3.3) at the highest concentration (10 μM). As well, complex **45** exhibited a limited phototoxicity againt certain cell lines (A431, for A253 and CAL27 see S3.3). This lower phototoxicity of the complexes with polar substituents is a little bit counter-intuitive as often polar substitution, like OH groups, increases the PDT effect, as it increases the solubility in the cellular surrounding.[31,58]

The 1,3,7,9-tetramethyl-5-pentafluorophenyl-substituted complex **50** (substituent in blue color in Figure 5, and S3.3) exhibited a high phototoxic activity against all cell lines at the concentration of 10 μM. Moreover, complex **50** exhibited a high phototoxicity already at 2 μM for specific cell lines (A431, for A253 see S3.3). Whereas the corresponding 1,3,7,9-tetramethyl-5-(4-fluoro-3-nitrophenyl)-substituted complex **51** (substituent in blue color in Figure 5 and S3.3) exhibited no significant phototoxicity. There is a tendency for the tetrafluorophenyl-substituted complexes to have a higher phototoxic activity than the corresponding 3-nitrophenyl-substituted compounds. This has also been observed for boron-dipyrromethene complexes with these substitutions.[28e] In other cases, (pentamethylcyclopentadienyl)iridium(III) complexes have also shown a high potential as anticancer agents.[8b,59] However, only a limited number of these (pentamethylcyclopentadienyl)iridium(III) complexes showed a significant *phototoxic* activity against cell lines.[18e,60]

Next, the (dipyrrinato)bis(2-phenylpyridyl)iridium(III) complexes (**52**–**71**) were as well tested against the cell lines (Figure 6, Figure 7, and S3.4 in the Supporting Information). Again, the complexes tested showed no significant dark toxici-

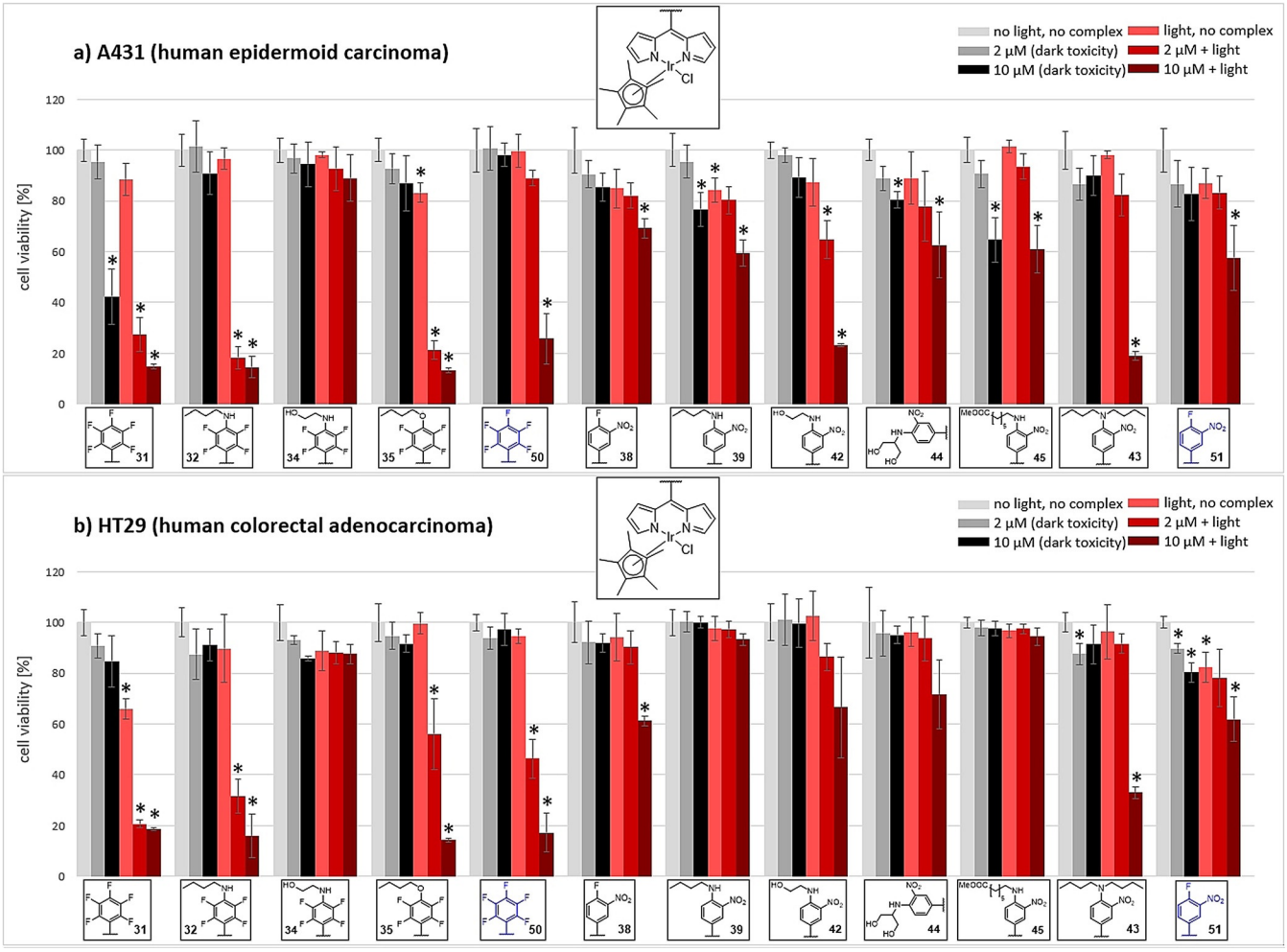

Figure 5. Dark and phototoxicity of chlorido(dipyrrinato)(pentamethylcyclopentadienyl)iridium(III) complexes in cellular assays with the A431 cell line (**a**) and the cell line HT29 (**b**). Blue colored structures **50** and **51** represent the two (pentamethylcyclopentadienyl)(1,3,7,9-tetramethyl-dipyrrinato)iridium(III) complexes.* indicates significant values with $p < 0.005$.

ty, except for the glycosylated conjugates **68**–**71** in the high concentration of 10 μM. The (dipyrrinato)bis(2-phenylpyridyl)iridium(III) compounds with polar substituents (**56**, **64**, and **65**), specifically the glycosylated conjugates **68**–**71** exhibited a very high phototoxicity even at a concentration of 2 μM.

A high phototoxic activity against cells has also been reported for some other types of (2-phenylpyridyl)iridium(III) complexes.[18d,61] No significant phototoxic activity was observed for the unfunctionalized complex **52** and the 3-nitrophenyl-substituted complexes **61**, **53**, and **66**, the other complexes exhibited a limited phototoxicity in some cell lines. Again, there is a tendency for the tetrafluorophenyl-substituted complexes to have a higher phototoxic activity than the corresponding 3-nitrophenyl-substituted compounds.

In order to evaluate the antimicrobial activity of the synthesized heteroleptic (dipyrrinato)iridium(III) complexes, bacterial assays against *S. aureus* and *P. aeruginosa* were performed with and without irradiation. The Gram-positive germ *S. aureus* is an important target as it is a typical member of the microflora of chronically infected wounds with a high tendency to develop antibiotic resistance.[62] Wound healing and treatment are prospective fields where aPDI has already shown potential.[63] The Gram-negative germ *P. aeruginosa* also has a high tendency to develop antibiotic resistance and is a major threat in nosocomial infections.[64] A critical aspect of the use of new antimicrobials in the clinical practice is that the drug candidates must be active in the presence of body fluids in complex biological environments. In addition, protein-rich environments can significantly influence the effectiveness of photosensitizers.[65] Therefore, to establish a more realistic model of the environment additional bacterial tests were performed in PBS supported with horse serum (10%). The bacterial assays included different conditions (blank: no complex and without illumination; identification of dark toxicity with 100 μM of the complex; and using different concentrations of 1, 10, and 100 μM, with and without addition of serum). To study the phototoxic activity against the bacteria, the corresponding complexes were incubated with cultures of *S. aureus* and *P. aeruginosa* (in the three different concentrations) for 30 min in PBS and in PBS supported with serum. Afterwards, the samples were exposed to white light with a power density and irradiation time resulting in an energy fluence of about 100 $J\,cm^{-2}$. The control experiment

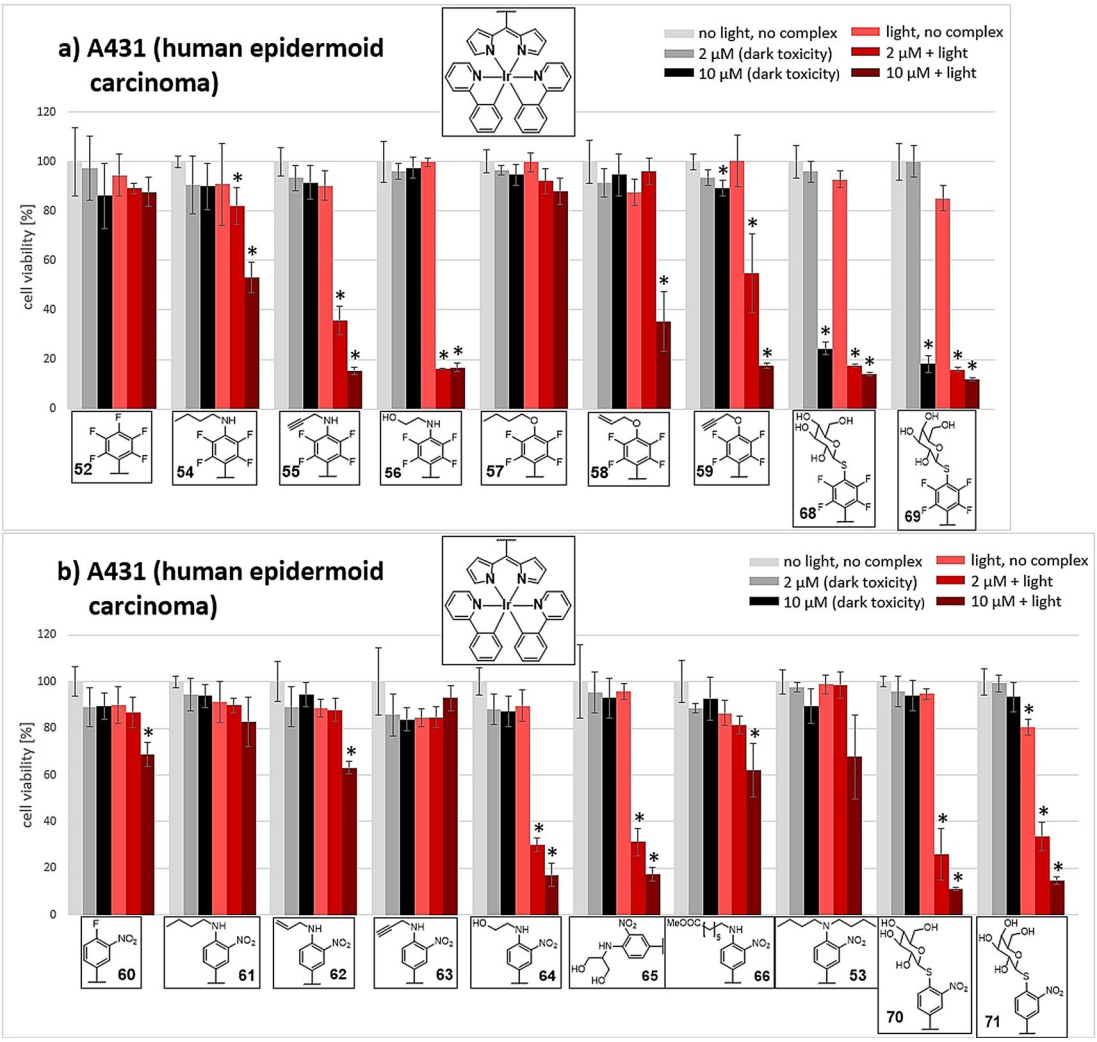

Figure 6. Dark and phototoxicity against the A431 cell line in cellular assay with bis(2-phenypyridyl)(tetrafluorophenyl-dipyrrinato)iridium(III) complexes (**a**) and (3-nitrophenyl-dipyrrinato)bis(2-phenypyridyl)iridium(III) complexes (**b**).* indicates significant values with $p < 0.005$.

with both bacterial strains treated only with this light dose can be found in the Supporting Information (S3.7). For the bacterial assays, an incubation time of 30 min was chosen. This short incubation time—compared to the incubation time for the investigations of the phototoxicity against the tumor cells (24 h)—was selected with respect to the specific recommendations of antibacterial therapy: Typically, bacterial reproduction is more rapid than that of cells, therefore, activity is needed after shorter residence times.[66] The antimicrobial activity of the (dipyrrinato)iridium(III) complexes is presented in Figure 8–10 (see also Supporting Information, S3.5, and S3.6) and the bacterial inactivation is given as the logarithm of the number of colony-forming units, lg (CFU mL^{-1}). In this context it should be taken into account that only a reduction of bacterial growth of at least 99.9 % ($\geq$ 3 log stages) is considered relevant with respect to bactericidal activity and a reduction by 4 and 5 log stages, respectively, is usually required for disinfectants in standard testing.[66c–f] Results for the series of chlorido(dipyrrinato)(pentamethylcyclopentadienyl)iridium(III) against *S. aureus* are presented in Figure 8. Almost all tested complexes suppressed bacterial growth below the detection limit at all three concentrations, that is, the number of bacteria becoming so low that no colonies were detected after incubation on the culture plates. Most likely, a light-independent antibacterial effect contributes to this as all compounds, except **50** and **51**, with the 1,3,7,9-tetramethyl-dipyrrinato ligand, exhibited strong dark toxicity in the control experiment with incubation of 100 μM of the complex. Such an antibacterial activity without irradiation, that is, an antibiotic effect, has also been observed for other selected iridium(III) complexes.[67] The complexes tested (**31**, **32**, **34**, **35**, **38**, **39**, and **42**–**45**), whether based on the 2,3,4,5-tetrafluorophenyl or the 3-nitrophenyl moiety, gave complete inactivation of *S. aureus* already at a concentration of 1 μM under light. Compounds **50** and **51** which showed no dark toxicity had nevertheless a strong phototoxic effect. A complete inactivation of bacteria was observed with **50** already at a concentration of 1 μM under light, while the corresponding complex **51** showed a complete photoinactivation of bacteria at a concentration of 10 μM.

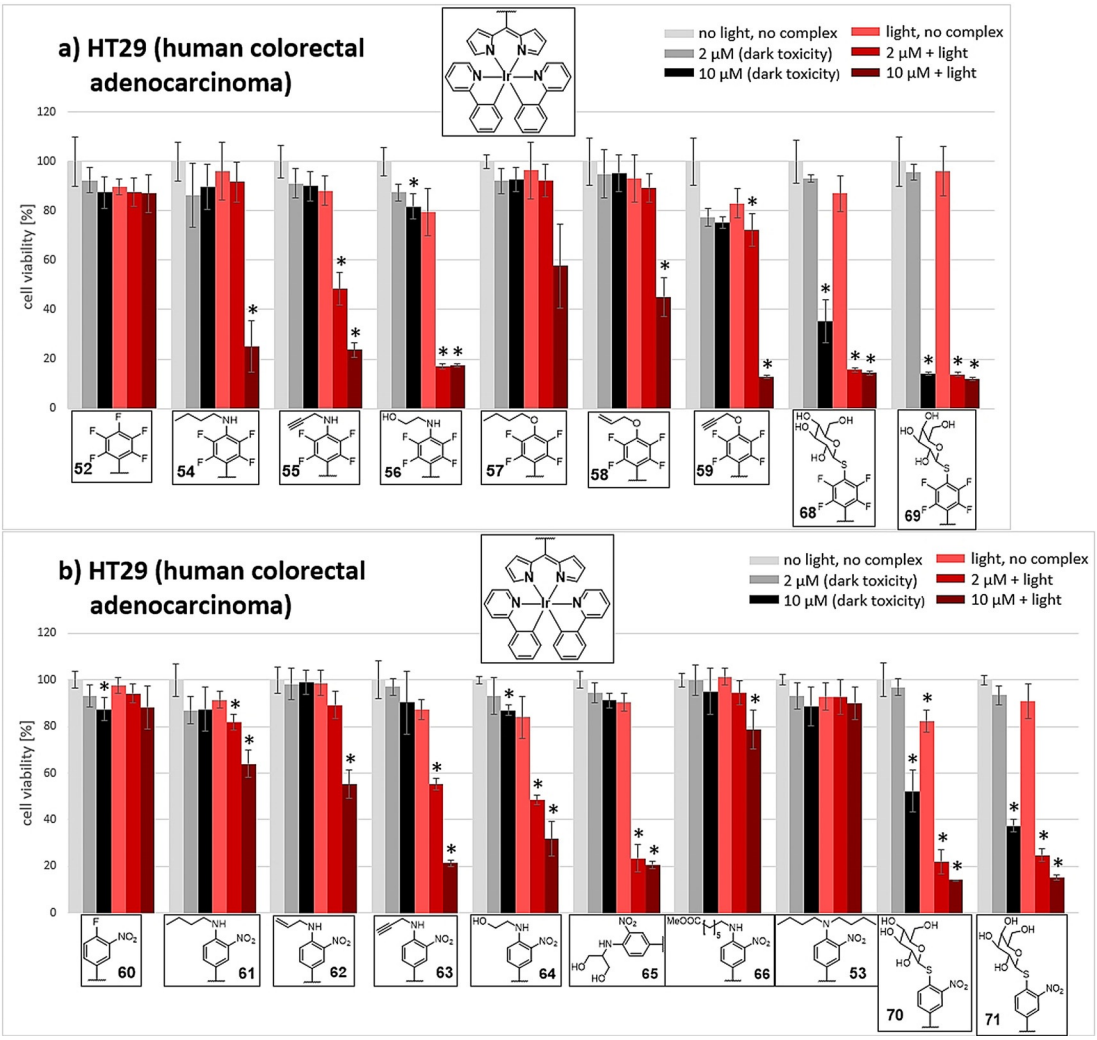

Figure 7. Dark and phototoxicity against the HT29 cell line in cellular assay with bis(2-phenypyridyl)(tetrafluorophenyl-dipyrrinato)iridium(III) complexes (**a**) and (3-nitrophenyl-dipyrrinato)bis(2-phenypyridyl)iridium(III) complexes (**b**).* indicates significant values with $p < 0.005$.

Next, these highly effective complexes were challenged in antibacterial tests in the presence of 10% serum (Figure 8b). Not unexpectedly, the effectiveness of the tested complexes decreased in the presence of serum. Nevertheless, in the presence of serum some complexes still exhibited strong dark and phototoxic effects against *S. aureus*. Complexes **31**, **32**, **35**, and **43** showed no change in their dark toxicity. For complexes **32** and **35** no differences in their activity against *S. aureus* were found in the presence of serum and in PBS alone, in both cases a complete inactivation even at the lowest concentration (1 μM) is observed. Notably, compounds **31** and **45** exhibited a phototoxic activity at the medium concentration (10 μM). As well, the 3-nitrophenyl-substituted complexes **39** and **43** showed a complete inactivation of the bacteria at the highest concentration (100 μM) under irradiation. In the case of the tetramethyldipyrrinato complexes **50** and **51**, only **50** still exhibited its phototoxic activity. Here, an effective inactivation of the bacteria was observed at 10 μM. This combined cytotoxic and phototoxic activity against bacteria has also been reported in some other cases for iridium(III) complexes.[18c,19] Again, there is a tendency for the tetrafluorophenyl-substituted complexes to have a higher phototoxic activity than the corresponding 3-nitrophenyl-substituted compounds in the presence of serum, as it was also observed in the cancer cell assays. Figure 9 shows the results of the chlorido(dipyrrinato)(pentamethylcyclopentadienyl)iridium(III) complexes against the Gram-negative Germ *P. aeruginosa*.

Compared to the results with *S. aureus*, the phototoxicity is significantly lower against *P. aeruginosa*. However, a reduction of bacterial growth of about 1.5 to 2 log stages was already achieved without light (100 μM) with the complexes **31**, **32**, **35**, **39**, **42**, and **45**. Such an antibacterial activity without irradiation has as well been observed for some other iridium(III) complexes.[9b,68] Here, however, a *phototoxic* reduction of bacterial growth below the detection limit was achieved with several complexes. A complete inactivation of *P. aeruginosa* was observed with the complexes **31**, **35**, **38**, **39**, and **45** already at a concentration of 10 μM under irradiation with light. In addition, the complexes **32**, **42**, and **44** showed a complete photoinactivation of *P. aeruginosa* at the highest concentration (100 μM).

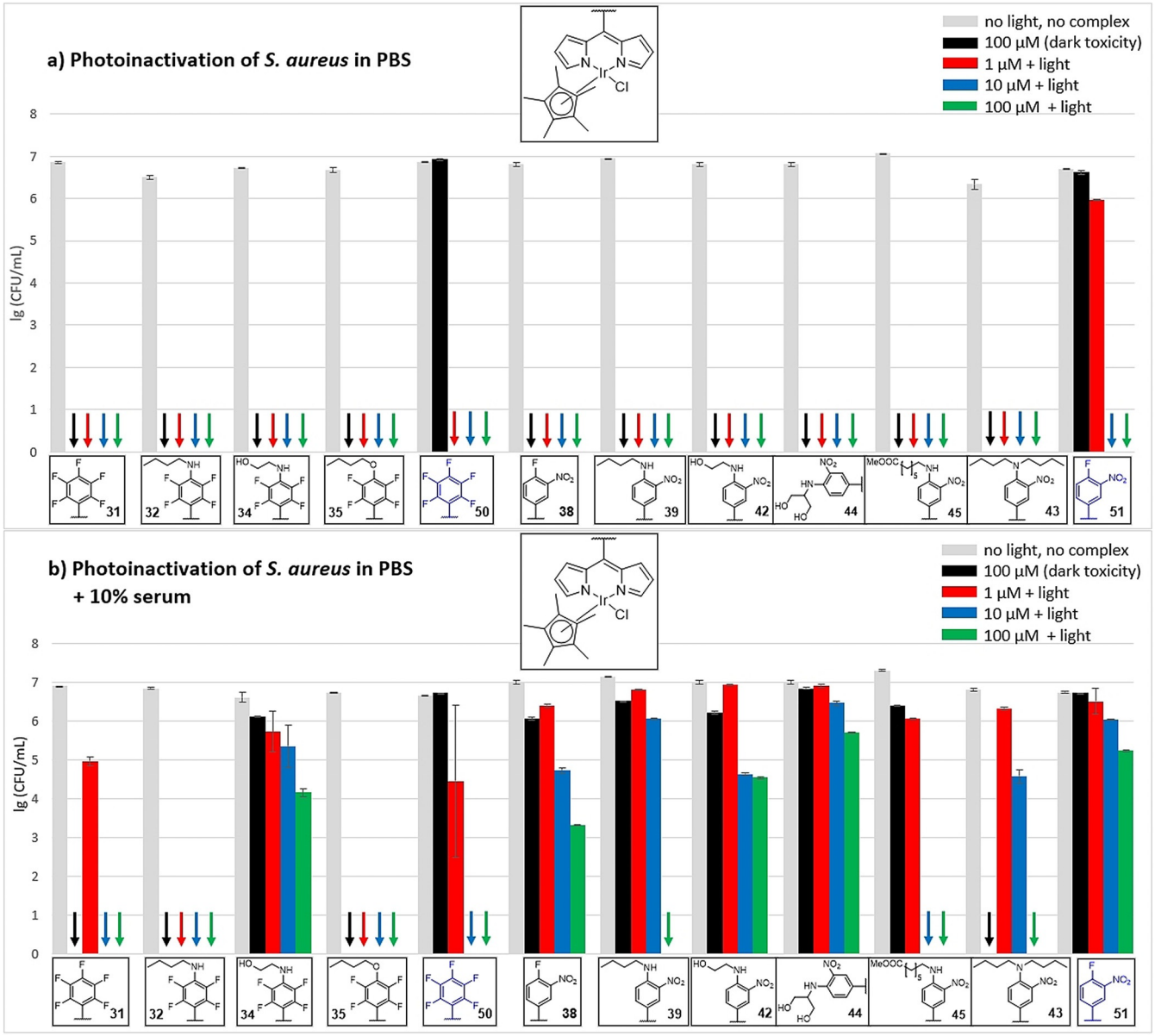

Figure 8. Photoinactivation of *S. aureus* by chlorido(dipyrrinato)(pentamethylcyclopentadienyl)iridium(III) complexes (30 min incubation and irradiation with white light) in phosphate-buffered saline (PBS) (**a**) and in PBS + 10% serum (**b**). The antibacterial toxicity is expressed as logarithm of the number of colony-forming units, lg (CFU mL^{-1}). Arrows indicate a suppression of bacterial growth below the detection limit. Blue colored structures **50** and **51** represent the two (pentamethylcyclopentadienyl(1,3,7,9-tetramethyl-dipyrrinato)iridium(III) complexes.

The 1,3,7,9-tetramethyl-dipyrrinato complexes **50** and **51** exhibited no dark or phototoxicity against *P. aeruginosa*. The lower antibacterial activity of the complexes against *P. aeruginosa* is not unexpected because Gram-negative germs are generally more difficult to be inactivated than Gram-positive ones. This is *i.a.* due to the pronounced differences in their cell wall composition.[65b,69] In fact, it is somewhat remarkable that some of the (dipyrrinato)(pentamethylcyclopentadienyl) complexes show such a pronounced activity against *P. aeruginosa* in PBS though they are not cationic, which is a typical feature found in photosensitizers active against Gram-negative bacteria.[69,70] However, this also gives cationic photosensitizers a higher affinity towards DNA rendering some of them potentially mutagenic.[71] Hence, compounds active against Gram-negative bacteria lacking cationic charges are desirable. Similar to the investigation with *S. aureus* the (dipyrrinato)(pentamethylcyclopentadienyl) complexes were finally challenged in their antibacterial activity against *P. aeruginosa* by performing the test in the presence of serum (Figure 9b). In many cases this antibacterial activity greatly decreased or vanished completely in the presence of serum. However, some complexes still exhibited a phototoxic effect on *P. aeruginosa* in the presence of serum. Complex **42** still showed a phototoxic effect with a reduction of about 2 log stages with light. While **31**, **35**, and **44** reduced the bacterial growth by about 1 log stage. Nevertheless, the observed antibacterial activities of the (dipyrrinato)(pentame-

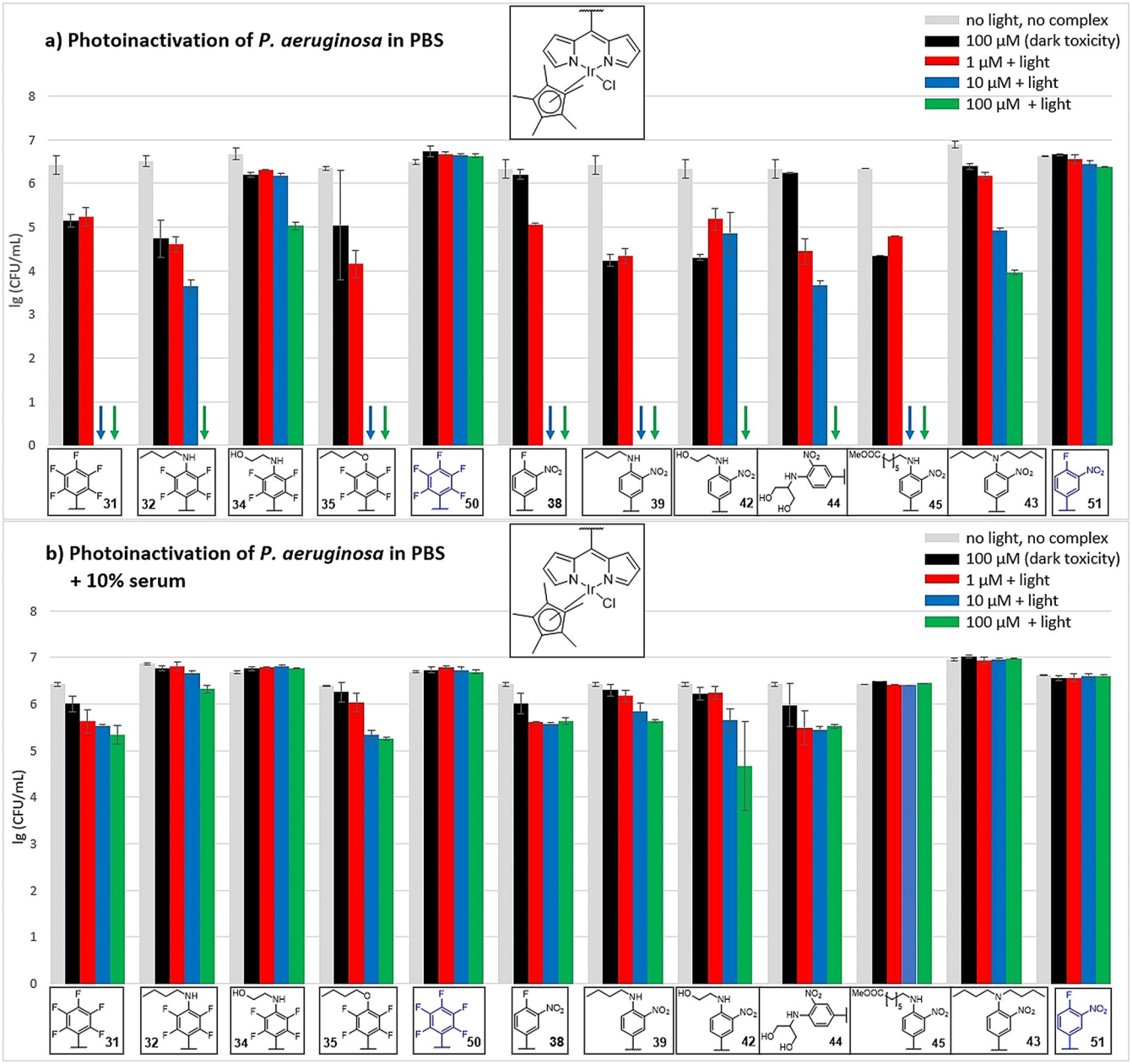

Figure 9. Photoinactivation of *P. aeruginosa* by chlorido(dipyrrinato)(pentamethylcyclopentadienyl)iridium(III) complexes (30 min incubation and irradiation with white light) in phosphate-buffered saline (PBS) (**a**) and in PBS + 10% serum (**b**). The antibacterial toxicity is expressed as logarithm of the number of colony-forming units, lg (CFU mL^{-1}). Arrows indicate a suppression of bacterial growth below the detection limit. Blue colored structures **50** and **51** represent the two (pentamethylcyclopentadienyl) (1,3,7,9-tetramethyl-dipyrrinato)iridium(III) complexes.

thylcyclopentadienyl) complexes against *S. aureus* and *P. aeruginosa* with and without illumination suggest that these compounds are valuable targets for more detailed QSAR studies on their (photo)antibiotic properties.

The (dipyrrinato)bis(2-phenylpyridyl)iridium(III) complexes were also tested against *S. aureus* and *P. aeruginosa* (Figure 10 and section S3.5, Supporting Information). The glycosylated conjugates **68**–**71** and the polar substituted complexes **56**, **64**, and **65** showed a very effective inactivation of *S. aureus* in PBS with a suppression of bacterial growth below the detection limit already at a concentration of 1 µM under light.

However, the tetrafluorophenyl-based complexes **56**, **68**, and **69** did exhibit a strong dark toxicity with a complete inactivation of bacteria already at a concentration of 100 µM.

The complexes **57**, **60**, and **66** exhibited a phototoxic activity, with complete inactivation of *S. aureus* at the highest concentration (100 µM) under light irradiation. The other 2,3,5,6-tertrafluorophenyl-based complexes (**52**, **55**, **58**, and **59**) provided an inactivation of *S. aureus* of at least 2 log stages at the highest concentration. While the other 3-nitrophenyl-based complexes (**53**, and **61**–**63**) showed no significant effect on *S. aureus*.

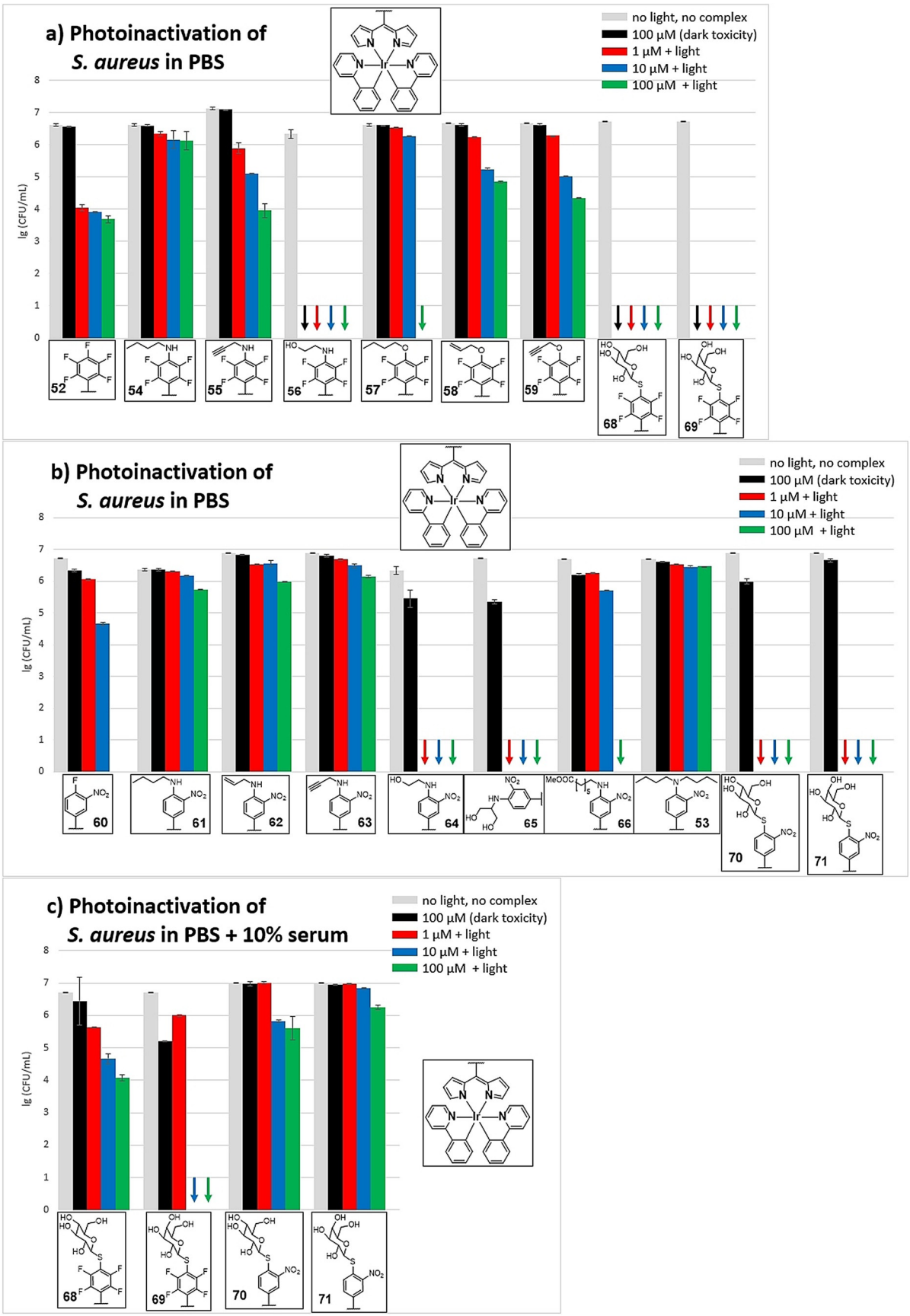

Figure 10. Photoinactivation of *S. aureus* (30 min incubation and irradiation with white light) by bis(2-phenylpyridyl)(tetrafluorophenyldipyrrinato)iridium(III) complexes in phosphate-buffered saline (PBS) (**a**), (3-nitrophenyldipyrrinato)bis(2-phenylpyridyl)iridium(III) complexes in PBS (**b**), and glycosylated (dipyrrinato)bis(2-phenylpyridyl)iridium(III) complexes in PBS + 10% serum (**c**). The antibacterial toxicity is expressed as logarithm of the number of colony-forming units, lg (CFU mL^{-1}). Arrows indicate a suppression of bacterial growth below the detection limit.

The tests with the (dipyrrinato)bis(2-phenylpyridyl)iridium(III) complexes on *S. aureus* were then repeated in the presence of serum. In most cases the antibacterial activity greatly decreased or vanished completely. In the case of the complexes with ligands carrying polar substituents polar-substituted complexes (**56**, **64**, and **65**) and complexes with glycosylated ligands (**70** and **71**), a reduction of bacterial growth of about one log stage was observed. Only the glycosylated 2,3,5,6-tetrafluorophenyl-substituted complexes, **68** and **69**, gave a significant reduction of the bacterial growth, with **69** being the most effective compound able to suppress bacterial growth below the detection limit.

Tests of the (dipyrrinato)bis(2-phenylpyridyl)iridium(III) complexes against *P. aeruginosa* revealed no significant phototoxicity or dark toxicity (see Supporting Information, S3.6).

Conclusions

In this work, synthetic strategies to (dipyrrinato)iridium(III) complexes carrying a multitude of functional groups were presented. Their potential for antitumor and antibacterial phototherapy has been preliminarily assessed in assays with four tumor cell lines, and two bacterial strains known to pose one major problem in nosocomial infections, the Gram-positive germ *S. aureus* and the Gram-negative germ *P. aeruginosa*. Starting point for the stepwise synthesis of the chlorido(dipyrrinato)(pentamethyl-η^5-cyclopentadienyl)iridium(III) complexes and the (dipyrrinato)bis(2-phenylpyridyl)iridium(III) complexes were *meso*-substituted dipyrrins, based on the pentafluorophenyl and the 4-fluoro-3-nitrophenyl moiety. As shown previously, the pentafluorophenyl and the 4-fluoro-3-nitrophenyl group can easily be modified by subsequent nucleophilic substitutions on their respective *para*-fluorine positions. Hence, the *p*-fluorine exchange with amines, alcohols and thio-carbohydrates was used to introduce specific functional structures. In addition to the synthesis of the cyclometalated iridium complexes via the complexation of pre-functionalized dipyrrins, the post-functionalization of the related pentafluorophenyl- and 4-fluoro-3-nitrophenyl-substituted dipyrrinato complexes was performed as well. This post-functionalization route proved to be especially suitable for introducing alkenyl and alkynyl as well as glyco-substituents, which are not accessible using the pre-functionalized dipyrrins. For several complexes, crystals suitable for X-ray crystal structure determination were obtained allowing to unequivocally determine their structure. These studies indicated that the molecular geometry of the dipyrrin ligand and immediate metal coordination environment was consistent between the phenylpyridine examples irrespective of the modification of the dipyrrin aryl unit. Flexion of the dipyrrin unit was observed when paired with the Cp* ligand complex, to accommodate the sterics of this ligand, increasing with additional steric bulk on the dipyrrin moiety.

In the preliminary assessment of their suitability for tumor (photo)therapy in assays against four cancer cell lines the non-functionalized chlorido(dipyrrinato)(pentamethylcyclopentadienyl)iridium(III) and the respective complexes carrying simple alkyl chains proved to be most effective.

In the tests with the (dipyrrinato)(2-phenylpyridyl)iridium(III) complexes the compounds having alkenyl, alkynyl, and polar (hydroxyl) substituents showed the strongest reduction of tumor cell viability, with the glyco-substituted complexes being most effective. In the evaluation of their antibacterial effect with and without light against the Gram-positive germ *S. aureus* the chlorido(dipyrrinato)(pentamethylcyclopentadienyl)iridium(III) complexes exhibited an exceptionally high toxicity with but also without illumination, regardless of the substitution.

On repetition of the test in the presence of serum strong dark and phototoxic effects were found for some compounds, namely the non-substituted and the simple alkyl-substituted ones. When testing the (dipyrrinato)(2-phenylpyridyl)iridium(III) complexes against *S. aureus* a high antibacterial activity was observed with the polar (hydroxyl) substituted compounds, specifically the glyco-modified complexes. Of these, the galactosyl-substituted complex (compound **69**) was also the only compound showing a bacterial reduction below the detection limit even in the presence of serum.

In the tests with the Gram-negative germ *P. aeruginosa*, again some of the chlorido(dipyrrinato)(pentamethylcyclopentadienyl)iridium(III)complexes were able to reduce bacterial growth to the limit of detection. And even in the presence of serum these complexes exerted a significant effect by reducing bacterial growth by one or two log stages. With the (dipyrrinato)(2-phenylpyridyl)iridium(III) complexes no significant antibacterial activity towards *P. aeruginosa* was found.

In summary, the synthetic tools provided herein, specifically the *post*-functionalization of fluorophenyl-substituted dipyrrinato-iridium complexes allow a convenient access to various functionalized cyclometalated iridium complexes. Some of these complexes are found to show a high phototoxicity against tumor cells and a strong antibacterial activity, often even without illumination. Of specific interest is the strong antibacterial activity of the chlorido(dipyrrinato)(pentamethylcyclopentadienyl)iridium(III) complexes against the Gram-positive germ *S. aureus* and the Gram-negative *P. aeruginosa* and the high activity of the glyco-substituted iridium complexes against tumor cells and bacteria, underlining the potential that such complexes hold for (photo)medical applications. The observed antibacterial activities of the (dipyrrinato)(pentamethylcyclopentadienyl) complexes with and without illumination value more detailed structure–activity investigations including modified glyco-substitutions on the way to new (photo)antimicrobials.

Experimental Section

General remarks: All reactions were performed in standard round bottom flasks. Air sensitive reactions were carried out under an argon gas protecting atmosphere. Solvents DCM, *n*-pentane, and methanol were purchased and used as received. Other solvents were purchased and distilled at reduced pressure. Purchased chemicals were used as received without further purification. All liquid reagents were added through syringes. Reactions were monitored by thin-layer chromatography (Merck, TLC Silica gel

60 F_{254}. Flash column chromatography was performed on silica gel (Fluka silica gel 60 M, 40–63 μm). NMR spectra were recorded with JEOL ECX400, JEOL ECP500, Bruker Avance500, and JEOL ECZ600 instruments. Multiplicity of the signals was assigned as follows: s = singlet, br s = broad singlet, d = doublet, t = triplet, dd = doublet of doublets, dt = doublet of triplets, td = triplet of doublets, ddd = doublet of doublets of doublets, ddt = doublet of doublets of triplets, m = multiplet, m_c = centered multiplet. Chemical shifts are reported relative to $CDCl_3$ (^{1}H: δ = 7.26 ppm, ^{13}C: δ = 77.2 ppm), CD_2Cl_2 (^{1}H: δ = 5.32 ppm, ^{13}C: δ = 53.8 ppm), [D_8]THF (^{1}H: δ = 3.58 ppm, ^{13}C: δ = 67.6 ppm), [D_6]DMSO (^{1}H: δ = 2.50 ppm, ^{13}C: δ = 39.5 ppm). All ^{13}C NMR spectra are proton-decoupled and coupling constants are given in hertz (Hz). 2D spectra were measured for detailed peak assignments (COSY, HMBC, and HMQC). HRMS analyses were carried out on an Agilent Technologies 6210 ESI-TOF (electrospray ionization, time of flight) instrument. IR spectra were measured with a JASCO FT/IR 4100 spectrometer equipped with a PIKE MIRacle™ ATR instrument. UV/Vis spectra were recorded on a SPECORD S300 UV/Vis spectrometer (Analytic Jena) in quartz cuvettes (1 cm length). Absorption spectra of selected heteroleptic (dipyrrinato)iridium(III) are given in the Supporting Information, section S13. Specified melting points were recorded on a Reichert Thermovar Apparatus and are not corrected.

Compounds **1**–**15**,[28a,b,d,e,33] **16**,[34] **18**,[27a] **20**–**22**,[27a] **24**,[28d] **25**,[33] **29**,[28d] **30**,[28d] and **72**[28b] were prepared according to the literature. Dipyrrins **16**, **18**, and **20**–**22** were previously synthesized via oxidation with DDQ.[27a,34] In this work the oxidation was performed with *p*-chloranil to increase the yield of the corresponding dipyrrins **16**, **18**, and **20**–**22**. Previously, dipyrrin **48** was described in the literature via one pot-multi-step synthesis,[38] herein, a stepwise synthesis of **48** is presented.

General synthetic procedure for the oxidation of dipyrromethanes (16–30): The corresponding dipyrromethane (**1**–**15**, 1 equiv.) was dissolved in THF and *p*-chloranil or DDQ (1 equiv, suspended in THF) was added. The reaction mixture was stirred for the indicated time at room temperature. Afterwards, the solvent was evaporated at reduced pressure, the remaining solid was dissolved and filtered over a silica gel filled glass frit. The filtrate was evaporated to dryness and purified by column chromatography.

General synthetic procedure for the chlorido(dipyrrinato)(pentamethyl-η^5-cyclopentadienyl)iridium(III) complexes (31–45): The corresponding dipyrrin (**16**–**30**, 1 equiv.) and the $[IrCl_2Cp^*]_2$ (0.5 equiv.) were dissolved in DCM or THF. DIPEA (14 equiv.) was added and the mixture was stirred for 24 h at room temperature. The flask was shielded from ambient light with aluminium foil. After the indicated time, saturated NaCl solution was added and extracted with DCM several times. The combined organic layers were dried with Na_2SO_4, filtered, and evaporated to dryness. The crude product was purified by column chromatography and recrystallized.

Preparation of chlorido(5-pentafluorophenyl-1,3,7,9-tetramethyldipyrrinato)(pentamethyl-η^5-cyclopentadienyl)iridium(III) (50): Dipyrrin 48 (250 mg, 0.68 mmol), $[IrCl_2Cp^*]_2$ (272 mg, 0.34 mmol) and DIPEA (1.62 mL, 9.55 mmol) were dissolved in 10 mL of THF. The mixture was stirred for 24 h at room temperature. The flask was shielded from ambient light with aluminium foil. After the indicated time, saturated NaCl solution was added and extracted with DCM several times. The combined organic layers were dried with Na_2SO_4, filtered, and evaporated to dryness. After column chromatography (silica gel, EtOAc/*n*-hexane = 1/1, v/v) and recrystallization (DCM/*n*-hexane) complex **50** was obtained as an orange-green solid (161 mg, 0.22 mmol, 32%). M.p. > 250 °C. ^{1}H NMR (500 MHz, CD_2Cl_2): δ (ppm) = 1.40 (s, 15H, Me_{Cp^*}), 1.68 (s, 6H, Me), 2.62 (s, 6H, Me), 6.16 (s, 2H, $H_{pyrrole}$). ^{13}C NMR (126 MHz, CD_2Cl_2): δ (ppm) = 8.6 (Me_{Cp^*}), 15.1 (Me), 18.9 (Me), 86.8 (C_{Cp^*}), 123.4 ($CH_{pyrrole}$), 130.6 (C_{meso}), 142.1 ($C_{pyrrole}$), 162.9 ($C_{pyrrole}$). ^{19}F NMR (376 MHz, CD_2Cl_2): δ (ppm) = −162.07—−161.89 (m, 2F, CF_{ortho}), −153.99 (t, J = 20.9 Hz, 1F, CF_{para}), −139.87 (dd, J = 24.3, 8.5 Hz, 1F, CF_{para}), −140.38 (dd, J = 51.5, 22.8 Hz, 2F, CF_{meta}). HRMS (ESI-TOF): *m/z* calcd for $C_{29}H_{29}F_5IrN_2^+$ $[M\text{-}Cl]^+$: 693.1875, found: 693.1857, *m/z* calcd for $C_{58}H_{58}ClF_{10}Ir_2N_4^+$ $[2M\text{-}Cl]^+$: 1421.3443, found: 1421.3393. UV/Vis (DCM): λ_{max} (nm) [log (ε L^{-1} mol^{-1} cm^{-1})] = 518 [4.62].

Preparation of chlorido(4-fluoro-3-nitrophenyl-1,3,7,9-tetramethyldipyrrinato)(pentamethyl-η^5-cyclopentadienyl)iridium(III) (51): Dipyrrin **49** (250 mg, 0.74 mmol), $[IrCl_2Cp^*]_2$ (293 mg, 0.37 mmol) and DIPEA (1.75 mL, 10.31 mmol) were dissolved in 10 mL of THF. The mixture was stirred for 24 h at room temperature. The flask was shielded from ambient light with aluminium foil. After the indicated time, saturated NaCl solution was added and extracted with DCM several times. The combined organic layers were dried with Na_2SO_4, filtered, and evaporated to dryness. After column chromatography (silica gel, DCM/EtOAc = 1/1, v/v) and recrystallization (DCM/*n*-hexane) complex **51** was obtained as a red-orange solid (137 mg, 0.20 mmol, 27%). M.p. > 250 °C. ^{1}H NMR (500 MHz, CD_2Cl_2): δ (ppm) = 1.41 (d, J = 5.4 Hz, 15H, Me_{Cp^*}), 1.48 (d, J = 2.3 Hz, 6H, Me), 2.60 (s, 6H, Me), 6.14 (d, J = 2.6 Hz, 2H, $H_{pyrrole}$), 7.43 (ddd, J = 24.4, 10.8, 8.5 Hz, 1H, Ar-H_{meta}), 7.57 (ddd, J = 8.4, 4.2, 2.1 Hz, 1H, Ar-H_{ortho}), 7.97 (td, J = 7.7, 7.2, 2.2 Hz, 1H, Ar-H_{ortho}). ^{13}C NMR (126 MHz, CD_2Cl_2): δ (ppm) = 9.0 (Me_{Cp^*}), 16.9 (Me), 18.7 (Me), 86.6 (C_{Cp^*}), 119.20 (d, J = 24.2 Hz, Ar-C_{meta}), 123.2 ($CH_{pyrrole}$), 126.50* (d, J = 2.4 Hz, Ar-C_{ortho}), 129.10 (d, J = 2.6 Hz,), 131.34 (d, J = 5.0 Hz, $C_{pyrrole}$), 136.14* (d, J = 8.6 Hz), 137.9 (Ar-C_{ortho}), 139.0 (C_{meso}), 143.40 (d, J = 5.7 Hz, $C_{pyrrole}$), 155.90 (d, J = 265.6 Hz, Ar-C_{para}), 162.0 ($C_{pyrrole}$). *These signals could not be assigned exactly to corresponding carbon atoms. They belong to the Ar-C_{ipso} and the Ar-C_{nitro} of the aryl moiety. ^{19}F NMR (376 MHz, CD_2Cl_2): δ (ppm) = −119.25–118.56 (m, 1F, CF). HRMS (ESI-TOF): *m/z* calcd for $C_{29}H_{32}FIrN_2O_2^+$ $[M\text{-}Cl]^+$: 666.2102, found: 666.2124. IR (ATR): myEqn.5 (cm^{-1}) = 3052 [ν(Ar-H)], 2960 and 2916 [ν(Me)], 1616 and 1580 [ν(C=C), ν(C=*N*-)], 1532 [ν_{as}(NO_2)], 1441 [δ(CH_2)], 1339 [ν_{sym}(NO_2)], 1087 [ν(C=CF)], 732 [δ(HC=CH)]. UV/Vis (DCM): λ_{max} (nm) [log (ε L^{-1} mol^{-1} cm^{-1})] = 509 [4.54].

General synthetic procedure for the (dipyrrinato)bis(2-phenylpyridyl)iridium(III) complexes (52–66): The corresponding dipyrrin (**16**–**30**, 1 equiv) and DIPEA (14 equiv) were dissolved in THF. Under an argon atmosphere the $[IrCl(ppy)_2]_2$ (0.5 equiv) was added and the mixture was stirred for 24 h under reflux. After the indicated time, DCM was added and washed with water several times. The organic layer was dried with Na_2SO_4, filtered, and evaporated to dryness. The crude product was purified by column chromatography and recrystallized.

General synthetic procedure for nucleophilic substitution of 52 with amines: Complex **52** (1 equiv) and the corresponding amine (20 equiv) were dissolved in DMSO. The mixture was stirred for 24 h at 80 °C. After the indicated time, the mixture was diluted with DCM and washed with water several times. The organic layer was dried with Na_2SO_4, filtered, and evaporated to dryness. The crude product was purified by column chromatography and recrystallization.

General synthetic procedure for nucleophilic substitution of 52 with alcohols: Complex **52** (1 equiv) was dissolved in THF, freshly powdered potassium hydroxide (5 equiv), and the corresponding alcohol (10 equiv) were added. The mixture was stirred for 24 h at room temperature. Afterwards, the mixture was diluted with DCM and washed several times with water. The organic layer was dried

with Na_2SO_4, filtered, and evaporated to dryness. The crude product was purified by column chromatography.

General synthetic procedure for nucleophilic substitution of 60 with amines: Complex **60** (1 equiv) and the corresponding amine (20 equiv) were dissolved in DCM. The mixture was stirred for 2 h at room temperature. After the indicated time, the mixture was diluted with EtOAc and washed with water several times. The organic layer was dried with Na_2SO_4, filtered, and evaporated to dryness. The crude product was purified by column chromatography.

General synthetic procedure for glycosylation of 52 and 60: The complex **52** or **60** (1 equiv) and the corresponding thio-carbohydrate sodium salt (1.2 equiv) were dissolved DMF. The mixture was stirred for the indicated time at room temperature. Afterwards, 5 mL of water was added and stirred for additional 5 min at room temperature. Due to the high polarity of the product, the mixture was directly evaporated to dryness with a rotary evaporator. The crude product was purified by column chromatography and recrystallization.

X-ray crystallography: The compounds **31**, **51**, **54**, **60** and **66** were each crystallized by slow evaporation of a solution of the target compound in dichloromethane (**31**, **60**), layered dichloromethane/hexane (**54**) or toluene (**51**, **66**) following the concept developed by Hope,[72] and the crystal structure obtained from patterns collected on a Bruker APEX-II Duo diffractometer with $Cu_{K\alpha}$ or $Mo_{K\alpha}$ as indicated in Table S1.1.1 Data reduction and multi-scan absorption corrections were applied with the Bruker APEX3 package.[73] Structures were solved using SHELXT,[74] and refinements were performed against $|F^2|$ using SHELXL in the ShelXle[75] GUI. All non-H atoms were refined with anisotropic thermal parameters, with H atoms as riding isotropic thermal parameters. C-bound H-positions were constrained to geometrically optimized positions, *N*-bound H atoms were positionally refined. Additional refinement details are presented in Supporting Information section S1.1.2.

Deposition numbers 2035034, 2035035, 2035036, 2035037, and 2035038 contain the supplementary crystallographic data for this paper. These data are provided free of charge by the joint Cambridge Crystallographic Data Centre and Fachinformationszentrum Karlsruhe Access Structures service www.ccdc.cam.ac.uk/structures.

Acknowledgements

The biolitec research GmbH gratefully acknowledges financial support by the German Bundesministerium für Bildung und Forschung (BMBF) (03ZZ0927B). This work has received funding from the European Union's Horizon 2020 research and innovation programme under the Marie Skłodowska–Curie Grant Agreement No. 764837 and through a grant from Science Foundation Ireland (IvP 13/IA/1894). It was prepared with the support of the Technical University of Munich—Institute for Advanced Study through a Hans Fischer Senior Fellowship for M.O.S. Open access funding enabled and organized by Projekt DEAL.

Conflict of interest

The authors declare no conflict of interest.

Keywords: (dipyrrinato)iridium(III) complexes · antimicrobial photodynamic inactivation · dipyrrins · glycosylation · photodynamic therapy

[1] a) M. Ohff, A. Ohff, M. E. van der Boom, D. Milstein, *J. Am. Chem. Soc.* **1997**, *119*, 11687–11688; b) M. Ohff, A. Ohff, D. Milstein, *Chem. Commun.* **1999**, 357–358; c) R. B. Bedford, S. M. Draper, P. N. Scully, S. L. Welch, *New J. Chem.* **2000**, *24*, 745–747.

[2] a) K.-C. Cheung, W.-L. Wong, D.-L. Ma, T.-S. Lai, K.-Y. Wong, *Coord. Chem. Rev.* **2007**, *251*, 2367–2385; b) C. Parmeggiani, F. Cardona, *Green Chem.* **2012**, *14*, 547–564.

[3] a) S. Elangovan, J. Neumann, J.-B. Sortais, K. Junge, C. Darcel, M. Beller, *Nat. Commun.* **2016**, *7*, 12641; b) J. J. Van Veldhuizen, J. E. Campbell, R. E. Giudici, A. H. Hoveyda, *J. Am. Chem. Soc.* **2005**, *127*, 6877–6882.

[4] a) S. H. Pine, G. S. Shen, H. Hoang, *Synthesis* **1991**, 165–166; b) R. R. Schrock, C. Czekelius, *Adv. Synth. Catal.* **2007**, *349*, 55–77; c) A. Fürstner, M. Liebl, C. W. Lehmann, M. Picquet, R. Kunz, C. Bruneau, D. Touchard, P. H. Dixneuf, *Chem. Eur. J.* **2000**, *6*, 1847–1857.

[5] a) G. Gasser, *Chimia* **2015**, *69*, 442–446; b) N. Muhammad, Z. Guo, *Curr. Opin. Chem. Biol.* **2014**, *19*, 144–153; c) I. Ott, R. Gust, *Arch. Pharm. Chem. Life Sci.* **2007**, *340*, 117–126; d) U. Ndagi, N. Mhlomgo, M. E. Soliman, *Drug Des. Dev. Ther.* **2017**, *11*, 599–616; e) P. Chellan, P. J. Sadler, *Chem. Eur. J.* **2020**, *26*, 8676–8688.

[6] a) D. E. Reichert, J. S. Lewis, C. J. Anderson, *Coord. Chem. Rev.* **1999**, *184*, 3–66; b) E. L. Que, C. J. Chang, *Chem. Soc. Rev.* **2010**, *39*, 51–60.

[7] M. Patra, G. Gasser, N. Metzler-Nolte, *Dalton Trans.* **2012**, *41*, 6350–6358.

[8] a) C. C. Konkankit, S. C. Marker, K. M. Knopf, J. J. Wilson, *Dalton Trans.* **2018**, *47*, 9934–9974; b) J. M. Gichumbi, H. B. Friedrich, *J. Organomet. Chem.* **2018**, *866*, 123–143; c) A. Zamora, G. Vigueras, V. Rodrígez, M. D. Santana, J. Ruiz, *Coord. Chem. Rev.* **2018**, *360*, 34–76; d) R. Guan, L. Xie, L. Ji, H. Chao, *Eur. J. Inorg. Chem.* **2020**, 3978–3986.

[9] a) V. Venkatesh, R. Berrocal-Martin, C. J. Wedge, I. Romero-Canelón, C. Sanchez-Cano, J.-I. Song, J. P. C. Coverdale, P. Zhang, G. J. Clarkson, A. Habtemariam, S. W. Magennis, R. J. Deeth, P. J. Sadler, *Chem. Sci.* **2017**, *8*, 8271–8278; b) T. Mukherjee, M. Mukherjee, B. Sen, S. Banerjee, G. Hundal, P. Chattopadhyay, *J. Coord. Chem.* **2014**, *67*, 2643–2660; c) J. J. Li, Z. Tian, Z. Xu, S. Zhang, Y. Feng, L. Zhang, Z. Liu, *Dalton Trans.* **2018**, *47*, 15772–15782; d) Y. Qi, Z. Liu, H. Li, P. J. Sadler, P. B. O'Connor, *Rapid Commun. Mass Spectrom.* **2013**, *27*, 2028–2032.

[10] a) S. Monro, K. L. Colón, H. Yin, J. Roque, III, P. Konda, S. Gujar, R. P. Thummel, L. Lilge, C. G. Cameron, S. A. McFarland, *Chem. Rev.* **2019**, *119*, 797–828; b) O. J. Stacey, S. J. A. Pope, *RSC Adv.* **2013**, *3*, 25550–25564; c) C. Imberti, P. Zhang, H. Huang, P. J. Sadler, *Angew. Chem. Int. Ed.* **2020**, *59*, 61–73; *Angew. Chem.* **2020**, *132*, 61–73; d) J. Li, L. Zeng, K. Xiong, T. W. Rees, C. Jin, W. Wu, Y. Chen, L. Ji, H. Chao, *Chem. Commun.* **2019**, *55*, 10972–10975; e) F. Heinemann, J. Karges, G. Gasser, *Acc. Chem. Res.* **2017**, *50*, 2727–2736; f) X. Tong, L. Zhang, L. Li, Y. Li, Z. Yang, D. Zhu, Z. Xie, *Dalton Trans.* **2020**, *49*, 11493–11497; g) P. Zhang, H. Huang, S. Banerjee, G. J. Clarkson, C. Ge, C. Imberti, P. J. Sadler, *Angew. Chem. Int. Ed.* **2019**, *58*, 2350–2354; *Angew. Chem.* **2019**, *131*, 2372–2376.

[11] a) P. Agostinis, K. Berg, K. A. Cengel, T. H. Foster, A. W. Girotti, S. O. Gollnick, S. M. Hahn, M. R. Hamblin, A. Juzeniene, D. Kessel, M. Korbelik, J. Moan, P. Mroz, D. Nowis, J. Piette, B. C. Wilson, J. Golab, *Ca-Cancer J. Clin.* **2011**, *61*, 250–281; b) D. E. J. G. J. Dolmans, D. Fukumura, R. K. Jain, *Nat. Rev. Cancer* **2003**, *3*, 380–387; c) Á. Juarranz, P. Jaén, F. Sanz-Rodríquez, J. Cuevas, S. González, *Clin. Transl. Oncol.* **2008**, *10*, 148–154; d) C.-M. Che, F.-M. Siu, *Curr. Opin. Chem. Biol.* **2010**, *14*, 255–261; e) S. B. Brown, E. A. Brown, I. Walker, *Lancet Oncol.* **2004**, *5*, 497–508.

[12] C. A. Robertson, D. Hawkins, E. H. Abrahamse, *J. Photochem. Photobiol., B* **2009**, *96*, 1–8.

[13] H. Huang, S. Banerjee, P. J. Sadler, *ChemBioChem* **2018**, *19*, 1574–1589.

[14] a) N. Kashef, Y.-Y. Huang, M. R. Hamblin, *J. Nanophotonics* **2017**, *6*, 853–879; b) T. Maisch, *J. Photochem. Photobiol. B* **2015**, *150*, 2–10; c) Y. Liu, R. Qin, S. A. J. Zaat, E. Breukink, M. Heger, *J. Clin. Transl. Res.* **2015**, *1*, 140–167; d) T. Maisch, *Mini-Rev. Med. Chem.* **2009**, *9*, 974–983.

[15] a) L. Costa, M. A. F. Faustino, M. G. P. M. S. Neves, Â. Cunha, A. Almeida, *Viruses* **2012**, *4*, 1034–1074; b) L. Sobotta, P. Skupin-Mrugalska, J. Mielcarek, T. Goslinski, J. Balzarini, *Mini-Rev. Med. Chem.* **2015**, *15*, 503–521;

c) A. Wiehe, J. M. O'Brien, M. O. Senge, *Photochem. Photobiol. Sci.* **2019**, *18*, 2565 – 2612.
[16] R. F. Donnelly, P. A. McCarron, M. M. Tunney, *Microbiol. Res.* **2008**, *163*, 1 – 12.
[17] a) M. S. Baptista, M. Wainwright, *Braz. J. Med. Res.* **2011**, *44*, 1 – 10; b) K. Page, M. Wilson, I. P. Parkin, *J. Mater. Chem.* **2009**, *19*, 3819 – 3831; c) K. Aponiene, E. Paskeviciute, I. Reklaitis, Z. Luksiene, *J. Food Eng.* **2015**, *144*, 29 – 35.
[18] a) S. K. Seth, P. Purkayastha, *Eur. J. Inorg. Chem.* **2020**, 2990 – 2997; b) C. Lu, S. Shah, B. Liu, W. Xu, L. Sun, S. Y. Qian, W. Sun, *ACS Appl. Bio Mater.* **2020**, *3*, 6865 – 6875; c) L. Wang, S. Monro, P. Cui, H. Yin, B. Liu, C. G. Cameron, W. Xu, M. Hetu, A. Fuller, S. Kilina, S. A. McFarland, W. Sun, *ACS Appl. Mater. Interfaces* **2019**, *11*, 3629 – 3644; d) J. Pracharova, G. Vigueras, V. Novohradsky, N. Cutillas, C. Janiak, H. Kostrhunova, J. Kasparkova, J. Ruiz, V. Brabec, *Chem. Eur. J.* **2018**, *24*, 4607 – 4619; e) C. Mari, H. Huang, R. Rubbiani, M. Schulze, F. Würthner, H. Chao, G. Gasser, *Eur. J. Inorg. Chem.* **2017**, 1745 – 1752.
[19] a) M. Valenzuela-Valderrama, V. Bustamante, N. Carrasco, I. A. González, P. Dreyse, C. E. Palavecino, *Photodiagn. Photodyn. Ther.* **2020**, *30*, 101662; b) E. Sauvageot, M. Elie, S. Gaillard, R. Daniellou, P. Fechter, I. J. Schalk, V. Gasser, J.-L. Renaud, G. L. A. Mislin, *Metallomics* **2017**, *9*, 1820 – 1827.
[20] a) D. F. Azar, H. Audi, S. Farhat, M. El-Sibai, R. J. Abi-Habib, R. S. Khnayzer, *Dalton Trans.* **2017**, *46*, 11529 – 11532; b) H. Chan, J. B. Ghrayche, J. Wei, A. K. Renfrew, *Eur. J. Inorg. Chem.* **2017**, 1679 – 1686.
[21] a) M. Yadav, A. K. Singh, D. S. Pandey, *J. Organomet. Chem.* **2011**, *696*, 758 – 763; b) M. Yadav, A. K. Singh, D. S. Pandey, *Organometallics* **2009**, *28*, 4713 – 4723; c) S. A. Baudron, *Dalton Trans.* **2020**, *49*, 6161 – 6175; d) R. S. Shikha Singh, R. P. Paitandi, R. K. Gupta, D. S. Pandey, *Coord. Chem. Rev.* **2020**, *414*, 213269. See also the classical examples: e) A. W. Johnson, I. T. Kay, *J. Chem. Soc.* **1961**, 2418 – 2423; f) M. Elder, B. R. Penfold, *J. Chem. Soc. A* **1969**, 2556 – 2559; g) F. A. Cotton, D. G. DeBoer, J. R. Pipal, *Inorg. Chem.* **1970**, *9*, 783 – 788; h) F. C. March, D. A. Couch, K. Emerson, J. E. Fergusson, W. T. Robinson, *J. Chem. Soc. A* **1971**, 440 – 448; i) H. Fischer, M. Schubert, *Ber. Dtsch. Chem. Ges.* **1924**, *57*, 610 – 617.
[22] a) J. R. Stork, V. S. Thoi, S. M. Cohen, *Inorg. Chem.* **2007**, *46*, 11213 – 11223; b) C. Brückner, V. Karunaratne, S. T. Rettig, D. Dolphin, *Can. J. Chem.* **1996**, *74*, 2182 – 2193; c) S. M. Cohen, S. R. Halper, *Inorg. Chim. Acta* **2002**, *341*, 12 – 16.
[23] a) D. Ramlot, M. Rebarz, L. Volker, M. Ovaere, D. Beljonne, W. Dahaen, L. Van Meervelt, C. Moucheron, A. K.-D. Mesmaeker, *Eur. J. Inorg. Chem.* **2013**, 2031 – 2040; b) M. Yadav, A. K. Singh, B. Maiti, D. S. Pandey, *Inorg. Chem.* **2009**, *48*, 7593 – 7603; c) R. P. Paitandi, R. S. Singh, S. Mukhopadhyay, G. Sharma, B. Koch, P. Vishnoi, D. S. Pandey, *Inorg. Chim. Acta* **2017**, *454*, 117 – 127.
[24] a) S. A. Baudron, *CrystEngComm* **2010**, *12*, 2288 – 2295; b) R. Matsuoka, T. Nabeshima, *Front. Chem.* **2018**, *6*, 349; c) Y.-F. Han, G.-X. Jin, *Chem. Soc. Rev.* **2014**, *43*, 2799 – 2823; d) J. Zhao, X. Zhang, L. Fang, C. Gao, C. Xu, S. Gou, *Small* **2020**, *16*, 2000363; e) R. Matsuoka, R. Toyoda, R. Sakamoto, M. Tsuchiya, K. Hoshiko, T. Nagayama, Y. Nonoguchi, K. Sugimoto, E. Nishibori, T. Kawai, H. Nishihara, *Chem. Sci.* **2015**, *6*, 2853 – 2858.
[25] a) G. Li, L. Ray, E. N. Glass, K. Kovnir, A. Khoroshutin, S. I. Gorelsky, M. Shatruk, *Inorg. Chem.* **2012**, *51*, 1614 – 1624; b) J. Sun, W. Wu, H. Gou, J. Zhao, *Eur. J. Inorg. Chem.* **2011**, 3165 – 3173.
[26] a) R. P. Paitandi, R. K. Gupta, R. S. Singh, G. Sharma, B. Koch, D. S. Pandey, *Eur. J. Med. Chem.* **2014**, *84*, 17 – 29; b) R. K. Gupta, A. Kumar, R. P. Paitandi, R. S. Singh, S. Mukhopadhyay, S. P. Verma, P. Das, D. S. Pandey, *Dalton Trans.* **2016**, *45*, 7163 – 7177.
[27] a) C. S. Gutsche, S. Gräfe, B. Gitter, K. J. Flanagan, M. O. Senge, N. Kulak, A. Wiehe, *Dalton Trans.* **2018**, *47*, 12373 – 12384; b) J. Karges, U. Basu, O. Blacque, H. Chao, G. Gasser, *Angew. Chem. Int. Ed.* **2019**, *58*, 14334 – 14340; *Angew. Chem.* **2019**, *131*, 14472 – 14478; c) S. Swavey, K. Morford, M. Tsao, K. Comfort, M. K. Kilroy, *J. Inorg. Biochem.* **2017**, *175*, 101 – 109.
[28] a) C. S. Gutsche, M. Ortwerth, S. Gräfe, K. J. Flanagan, M. O. Senge, H.-U. Reissig, N. Kulak, A. Wiehe, *Chem. Eur. J.* **2016**, *22*, 13953 – 13964; b) H. R. A. Golf, H.-U. Reissig, A. Wiehe, *Org. Lett.* **2015**, *17*, 982 – 985; c) Y. Volkova, B. Brizet, P. D. Harvey, F. Denat, C. Goze, *Eur. J. Org. Chem.* **2014**, 2268 – 2274; d) B. F. Hohlfeld, K. J. Flanagan, N. Kulak, M. O. Senge, M. Christmann, A. Wiehe, *Eur. J. Org. Chem.* **2019**, 4020 – 4033; e) B. F. Hohlfeld, B. Gitter, K. J. Flanagan, C. J. Kingsbury, N. Kulak, M. O. Senge, A. Wiehe, *Org. Biomol. Chem.* **2020**, *18*, 2416 – 2431.
[29] a) J. S. Smalley, M. R. Waterland, S. G. Telfer, *Inorg. Chem.* **2009**, *48*, 13 – 15; b) K. Hanson, A. Tamayo, V. V. Diev, M. T. Whited, P. I. Djurovich, M. E. Thompson, *Inorg. Chem.* **2010**, *49*, 6077 – 6084; c) J. D. Hall, T. M. McLean, S. J. Smalley, M. R. Waterland, S. G. Telfer, *Dalton Trans.*. **2010**, *39*, 437 – 445.
[30] K. Takaki, E. Sakuda, A. Ito, S. Horiuchi, Y. Arikawa, K. Umakoshi, *Inorg. Chem.* **2019**, *58*, 14542 – 14550.
[31] D. Samaroo, M. Vinodu, X. Chen, C. M. Drain, *J. Comb. Chem.* **2007**, *9*, 998 – 1011.
[32] a) N. T. Anderson, P. H. Dinolfo, X. Wang, *J. Mater. Chem. C* **2018**, *6*, 2452 – 2459; b) M. C. Bennion, M. A. Burch, D. G. Dennis, M. E. Lech, K. Neuhaus, N. L. Fendler, M. R. Parris, J. E. Cuadra, C. F. Dixon, G. T. Mukosera, D. N. Blauch, L. Hartmann, N. L. Snyder, J. V. Ruppel, *Eur. J. Org. Chem.* **2019**, 6496 – 6503; c) M. H. Staegemann, S. Gräfe, B. Gitter, K. Achazi, E. Quaas, R. Haag, A. Wiehe, *Biomacromolecules* **2018**, *19*, 222 – 238.
[33] C. S. Gutsche, B. F. Hohlfeld, K. J. Flanagan, M. O. Senge, N. Kulak, A. Wiehe, *Eur. J. Org. Chem.* **2017**, 3187 – 3196.
[34] L. Yu, K. Muthukumaran, I. V. Sazanovich, C. Kirmaier, E. Hindin, J. R. Diers, P. D. Boyle, D. F. Bocain, D. Holten, J. S. Lindsey, *Inorg. Chem.* **2003**, *42*, 6629 – 6647.
[35] a) S. F. Vyboishchikov, M. Bühl, W. Thiel, *Chem. Eur. J.* **2002**, *8*, 3962 – 3975; b) A. Fürstner, *Angew. Chem. Int. Ed.* **2013**, *52*, 2794 – 2819; *Angew. Chem.* **2013**, *125*, 2860 – 2887.
[36] a) M. B. France, J. Feldman, R. H. Grubbs, *J. Chem. Soc. Chem. Commun.* **1994**, 1307 – 1308; b) R. Ahuja, S. Kundu, A. S. Goldman, M. Brookhart, B. C. Vicenté, S. L. Scott, *Chem. Commun.* **2008**, 253 – 255; c) A. J. Nawara-Hultzsch, J. D. Hackenberg, B. Punji, C. Supplee, T. J. Emge, B. C. Bailey, R. R. Schrock, M. Brookhart, A. S. Goldman, *ACS Catal.* **2013**, *3*, 2505 – 2514.
[37] a) M. Tsuchiya, R. Sakamoto, M. Shimada, Y. Yoshinori, Y. Hattori, K. Sugimoto, E. Nishibori, H. Nishihara, *Inorg. Chem.* **2016**, *55*, 5732 – 5734; b) Q. Miao, J.-Y. Shin, B. O. Patrick, D. Dolphin, *Chem. Commun.* **2009**, 2541 – 2543; c) J. Karges, O. Blacque, H. Chao, G. Gasser, *Inorg. Chem.* **2019**, *58*, 12422 – 12432; d) R. Sakamoto, T. Iwashima, J. F. Kögel, S. Kusaka, M. Tsuchiya, Y. Kitagawa, H. Nishihara, *J. Am. Chem. Soc.* **2016**, *138*, 5666 – 5677; e) R. Toyoda, M. Tsuchiya, R. Sakamoto, R. Matsuoka, K.-H. Wu, Y. Hattori, H. Nishihara, *Dalton Trans.* **2015**, *44*, 15103 – 15106.
[38] X. Liu, H. Nan, W. Sun, Q. Zhang, M. Zhan, L. Zou, Z. Xie, X. Li, C. Lu, Y. Cheng, *Dalton Trans.* **2012**, *41*, 10199 – 10210.
[39] a) K. Jain, P. Kesharwani, U. Gupta, N. K. Jain, *Biomaterials* **2012**, *33*, 4166 – 4186; b) H. Zhang, Y. Ma, X.-L. Sun, *Med. Res. Rev.* **2010**, *30*, 585; c) S. V. Moradi, W. M. Hussein, P. Varamini, P. Simerska, I. Toth, *Chem. Sci.* **2016**, *7*, 2492 – 2500; d) E. Cho, S. Jung, *Molecules* **2015**, *20*, 19620 – 19646.
[40] a) R. Pretorius, J. Olguín, M. Albrecht, *Inorg. Chem.* **2017**, *56*, 12410 – 12420; b) M.-J. Li, P. Jiao, W. He, C. Yi, C.-W. Li, X. Chen, G.-N. Chen, M. Yang, *Eur. J. Inorg. Chem.* **2011**, 197 – 200; c) M. Felici, P. Contreras-Carballada, Y. Vida, J. M. M. Smits, R. J. M. Nolte, L. De Cola, R. M. Williams, M. C. Feiters, *Chem. Eur. J.* **2009**, *15*, 13124 – 13134.
[41] a) N. Shivran, M. Tyagi, S. Mula, P. Gupta, B. Saha, B. S. Padro, S. Chattopadhyay, *Eur. J. Med. Chem.* **2016**, *122*, 352 – 365; b) D. Lim, M. A. Brimble, R. Kowalczyk, A. J. A. Watson, A. J. Fairbanks, *Angew. Chem. Int. Ed.* **2014**, *53*, 11907 – 11911; *Angew. Chem.* **2014**, *126*, 12101 – 12105; c) S. Bhatia, M. Dimde, R. Haag, *Med. Chem. Commun.* **2014**, *5*, 862 – 878; d) T. Papalia, A. Barattucci, S. Campagna, F. Puntoriero, T. Salerno, P. Bonaccorsi, *Org. Biomol. Chem.* **2017**, *15*, 8211 – 8217.
[42] a) R. Klingenburg, C. B. W. Stark, A. Wiehe, *Org. Lett.* **2019**, *21*, 5417 – 5420; b) S. Singh, A. Aggarwal, S. Thompson, J. P. C. Tomé, X. Zhu, D. Samaroo, M. Vinodu, R. Gao, C. M. Drain, *Bioconjugate Chem.* **2010**, *21*, 2136 – 2146; c) F. Faschinger, S. Aichhorn, M. Himmelsbach, W. Schoefberger, *Synthesis* **2014**, *46*, 3085 – 3096.
[43] X. Chen, L. Hui, D. A. Foster, C. M. Drain, *Biochemistry* **2004**, *43*, 10918 – 10929.
[44] a) J. M. Zimbron, K. Passador, B. Gatin-Fraudet, C.-M. Bachelet, D. Plażuk, L.-M. Chamoreau, C. Botuha, S. Thorimbert, M. Salmain, *Organometallics* **2017**, *36*, 3435 – 3442; b) B. Liu, S. Monro, M. J. Jabed, C. G. Cameron, K. L. Colón, W. Xu, S. Kilina, S. A. McFarland, W. Sun, *Photochem. Photobiol. Sci.* **2019**, *18*, 2381 – 2396; c) G. Gupta, P. Kumari, J. Y. Ryu, J. Lee, S. M. Mobin, C. Y. Lee, *Inorg. Chem.* **2019**, *58*, 8587 – 8595; d) G. Gupta, S. Cherukommu, G. Srinivas, S. W. Lee, S. H. Mun, J. Jung, N. Nagesh, C. Y.

Lee, *J. Inorg. Biochem.* **2018**, *189*, 17 – 29; e) R. P. Paitandi, S. Mukhopadhyay, R. S. Singh, V. Sharma, S. M. Mobin, D. S. Pandey, *Inorg. Chem.* **2017**, *56*, 12232 – 12247; f) L. Tabrizi, H. Chiniforoshan, *RSC Adv.* **2017**, *7*, 34160 – 34169.
[45] a) H. R. A. Golf, H.-U. Reissig, A. Wiehe, *Eur. J. Org. Chem.* **2015**, 1548 – 1568; b) P. K. B. Palomaki, P. H. Dinolfo, *ACS Appl. Mater. Interfaces* **2011**, *3*, 4703 – 4713; c) M. D. Yilmaz, O. A. Bozdemir, E. U. Akkaya, *Org. Lett.* **2006**, *8*, 2871 – 2873.
[46] Z. Liu, P. J. Sadler, *Acc. Chem. Res.* **2014**, *47*, 1174 – 1185.
[47] C. R. Groom, I. J. Bruno, M. P. Lightfoot, S. C. Ward, *Acta Crystallogr. Sect. B* **2016**, *72*, 171 – 179.
[48] M. A. Filatov, S. Karuthedath, P. M. Polestshuk, S. Callaghan, K. J. Flanagan, T. Wiesner, F. Laquai, M. O. Senge, *ChemPhotoChem* **2018**, *2*, 606 – 615.
[49] R. K. Gupta, R. Pandey, G. Sharma, R. Prasad, B. Koch, S. Srikrishna, P. Z. Li, Q. Xu, D. S. Pandey, *Inorg. Chem.* **2013**, *52*, 3687 – 3698.
[50] N. Singh, J. H. Jo, Y. H. Song, H. Kim, D. Kim, M. S. Lah, K. W. Chi, *Chem. Commun.* **2015**, *51*, 4492 – 4495.
[51] T. Soya, A. Osuka, *Chem. Eur. J.* **2015**, *21*, 10639 – 10644.
[52] A. C. Carrasco, V. Rodríguez-Fanjul, A. Habtemariam, A. M. Pizarro, *J. Med. Chem.* **2020**, *63*, 4005 – 4021.
[53] S. Ladouceur, D. Fortin, E. Zysman-Colman, *Inorg. Chem.* **2010**, *49*, 5625 – 5641.
[54] S. J. Garden, J. L. Wardell, J. M. S. Skakle, J. N. Low, C. Glidewell, *Acta Crystallogr. Sect. C* **2004**, *60*, o328 – o330.
[55] C. Bronner, M. Veiga, A. Guenet, L. De Cola, M. W. Hosseini, C. A. Strassert, S. A. Baudron, *Chem. Eur. J.* **2012**, *18*, 4041 – 4050.
[56] C. Bronner, S. A. Baudron, M. W. Hosseini, *Inorg. Chem.* **2010**, *49*, 8659 – 8661.
[57] J. H. Hong, S. Kim, H. So, J. H. Lee, H. Hwang, K. M. Lee, *Dyes Pigments* **2020**, *183*, 108706.
[58] a) R. Bonnett, *Chem. Soc. Rev.* **1995**, *24*, 19 – 33; b) F. Li, Q. Liu, Z. Liang, J. Wang, M. Pang, W. Huang, W. Wu, Z. Hong, *Org. Biomol. Chem.* **2016**, *14*, 3409 – 3422; c) C. N. Lunardi, A. C. Tedesco, *Curr. Org. Chem.* **2005**, *9*, 813 – 821.
[59] a) Z. Liu, A. Habtemariam, A. M. Pizarro, S. A. Fletcher, A. Kisova, O. Vrana, L. Salassa, P. C. A. Bruijnincx, G. J. Clarkson, V. Brabec, P. J. Sadler, *J. Med. Chem.* **2011**, *54*, 3011 – 3026; b) J. M. Hearn, G. M. Hughes, I. Romero-Canelón, A. F. Munro, B. Rubio-Ruiz, Z. Liu, N. O. Carragher, P. J. Sadler, *Metallomics* **2018**, *10*, 93 – 107.
[60] L. Tabrizi, *Dalton Trans.* **2017**, *46*, 7242 – 7252.
[61] a) S. Yi, Z. Lu, J. Zhang, J. Wang, Z. Xie, L. Hou, *ACS Appl. Mater. Interfaces* **2019**, *11*, 15276 – 15289; b) J. S. Nam, M.-G. Kang, J. Kang, S.-Y. Park, S. J. C. Lee, H.-T. Kim, J. K. Seo, O.-H. Kwon, M. H. Lim, H.-W. Rhee, T.-H. Kwon, *J. Am. Chem. Soc.* **2016**, *138*, 10968 – 10977; c) F.-X. Wang, M.-H. Chen, Y.-N. Lin, H. Zhang, C.-P. Tan, L.-N. Ji, Z.-W. Mao, *ACS Appl. Mater. Interfaces* **2017**, *9*, 42471 – 42481.
[62] H. F. Chambers, F. R. DeLeo, *Nat. Rev. Microbiol.* **2009**, *7*, 629 – 641.
[63] a) D. Vecchio, T. Dai, L. Huang, L. Fantetti, G. Roncucci, M. R. Hamblin, *J. Biophotonics* **2013**, *6*, 733 – 742; b) X. Hu, Y.-Y. Huang, Y. Wang, X. Wang, M. R. Hamblin, *Front. Microbiol.* **2018**, *9*, 01299.
[64] a) Z. Pang, R. Raudonis, B. R. Glick, T.-J. Lin, Z. Cheng, *Biotechnol. Adv.* **2019**, *37*, 177 – 192; b) P. Pachori, R. Gothalwal, P. Gandhi, *Genes Dis.* **2019**, *6*, 109 – 119; c) F. Lucca, M. Guarnieri, M. Ros, G. Muffato, R. Rigoli, L. D. Dalt, *Clin. Respir. J.* **2018**, *12*, 2189 – 2196.
[65] a) T. Dai, Y. Y. Huang, M. R. Hamblin, *Photodiagn. Photodyn. Ther.* **2009**, *6*, 170 – 188; b) G. Jori, C. Fabris, M. Soncin, S. Ferro, O. Coppellotti, D. Dei, L. Fantetti, G. Chiti, G. Roncucci, *Lasers Surg. Med.* **2006**, *38*, 468 – 481; c) T. Dai, Y.-Y. Huang, S. K. Sharma, J. T. Hashmi, D. B. Kurup, M. R. Hamblin, *Recent Pat. Anti-Cancer Drug Discovery* **2010**, *5*, 124 – 151.
[66] a) L.-C. Lu, Y.-W. Chen, C.-C. Chou, *Int. J. Food Microbiol.* **2005**, *102*, 213 – 220; b) T. E. Shehata, A. G. Marr, *J. Bacteriol.* **1970**, *103*, 789 – 792; c) G. A. Pankey, L. D. Sabath, *Clin. Infect. Dis.* **2004**, *38*, 864 – 870; d) R. M. abd El-Baky, *Am. J. Microbiol. Res.* **2016**, *4*, 1 – 15; e) Bekanntmachung des Rober Koch-Institutes, *Bundesgesundheitsbl.* **2013**, *56*, 1696 – 1701; f) NCCLS. Methods for determining bactericidal activity of antibacterial agents; approved guideline. NCCLS document M26 A. Villanova, PA: NCCLS, 1999 and also EN 13727.
[67] a) F. Chen, J. Moat, D. McFeely, G. Clarkson, I. J. Hands-Portman, J. P. Furner-Pardoe, F. Harrison, C. G. Dowson, P. J. Sadler, *J. Med. Chem.* **2018**, *61*, 7330 – 7344; b) M. Pandrala, F. Li, M. Feterl, Y. Mulyana, J. M. Warner, L. Wallace, F. R. Keene, J. G. Collins, *Dalton Trans.* **2013**, *42*, 4686 – 4694; c) A. Lapasam, L. Dkhar, N. Joshi, K. M. Poluri, M. R. Kollipara, *Inorg. Chim. Acta* **2019**, *484*, 255 – 263; d) A. Gupta, P. Prasad, S. Gupta, P. K. Sasmal, *ACS Appl. Mater. Interfaces* **2020**, *12*, 35967 – 35976.
[68] Q.-Y. Yi, W.-Y. Zhang, M. He, F. Du, X.-Z. Wang, Y.-J. Wang, Y.-Y. Gu, L. Bai, Y.-J. Liu, *J. Biol. Inorg. Chem.* **2019**, *24*, 151 – 159.
[69] B. M. Amos-Tautua, S. P. Songca, O. S. Oluwafemi, *Molecules* **2019**, *24*, 2456.
[70] X. Ragàs, D. Sánchez-García, R. Ruiz-González, T. Dai, M. Agut, M. R. Hamblin, S. Nonell, *J. Med. Chem.* **2010**, *53*, 7796 – 7803.
[71] a) T. G. M. Smijs, M. J. M. Nivard, H. J. Schuitmaker, *Photochem. Photobiol.* **2004**, *79*, 332 – 338; b) R. A. Floyd, J. E. Schneider, Jr., D. P. Dittmer, *Antiviral Res.* **2004**, *61*, 141 – 151; c) J. M. Mundt, L. Rouse, J. Van den Bossche, R. P. Goodrich, *Photochem. Photobiol.* **2014**, *90*, 957 – 964; d) T. Qin, K. Liu, D. Song, C. Yang, H. Su, *Chem. Asian J.* **2017**, *12*, 1578 – 1586.
[72] a) H. Hope, *Progress in Inorganic Chemistry, Volume 41* (Ed.: K. D. Karlin), Wiley, **1994**, pp. 1 – 19; b) M. O. Senge, *Z. Naturforsch* **2000**, *55b*, 336 – 344.
[73] Bruker (2012), *APEX3*, Bruker AXS Inc., Madison, Wisconsin, USA.
[74] G. M. Sheldrick, *Acta Crystallogr. Sec. A* **2015**, *71*, 3 – 8.
[75] C. B. Hübschle, G. M. Sheldrick, B. Dittrich, *J. Appl. Crystallogr.* **2011**, *44*, 1281 – 1284.

Manuscript received: October 30, 2020
Revised manuscript received: November 24, 2020
Accepted manuscript online: November 25, 2020
Version of record online: February 9, 2021

